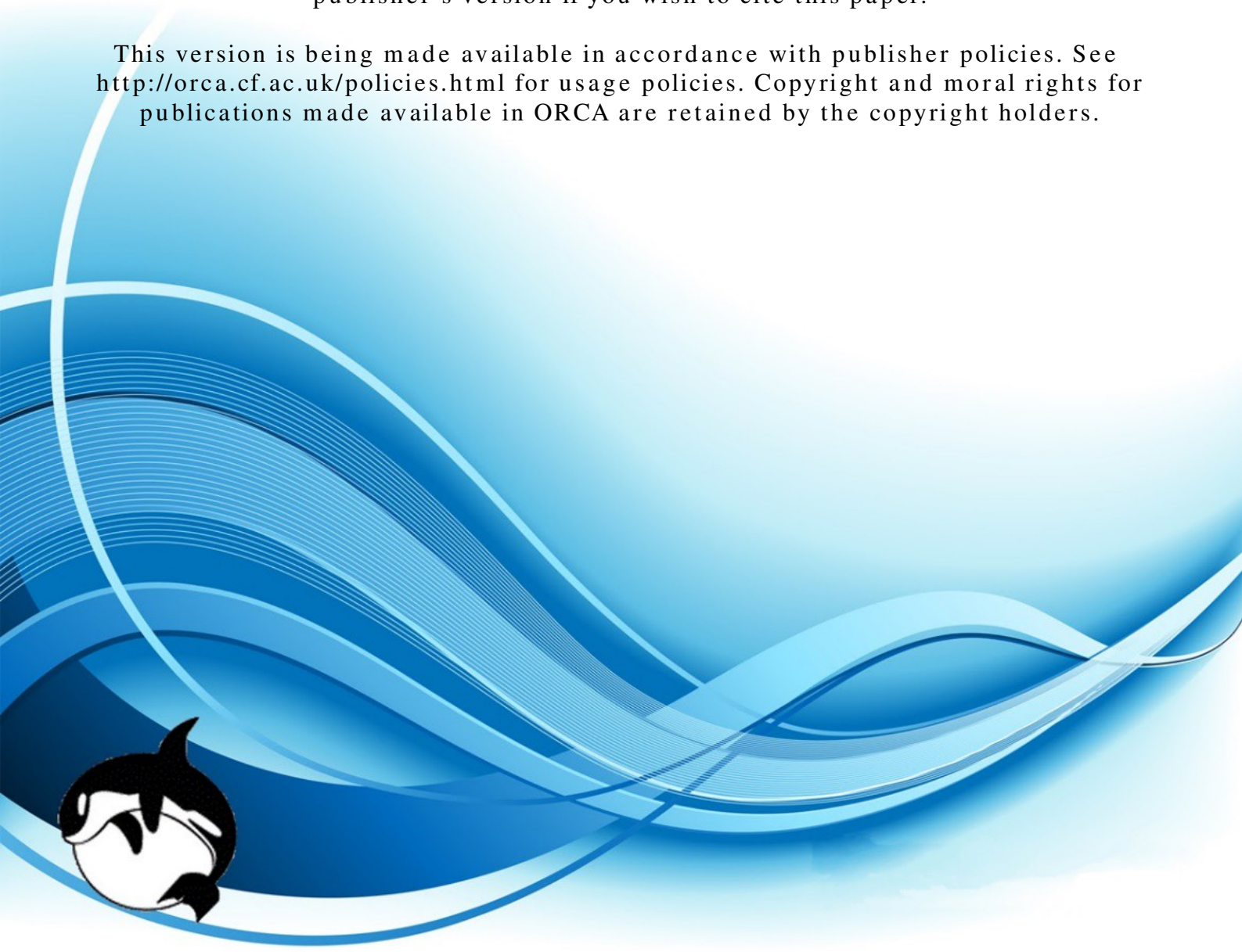

ROOTING PORTIONS OF A YOUNG PSEUDOSPOROCHNALEAN FROM THE CATSKILL DELTA COMPLEX OF NEW YORK

William E. Stein[1,*], Christopher M Berry[2,*], Linda VanAller Hernick[3] and Frank Mannolini[3]

[1]State University of New York, Binghamton, NY 13902-6000

[2]School of Earth and Ocean Sciences, Cardiff University, Cardiff CF10 3YE Wales, UK

[3]New York State Museum, Albany NY 12230

*Authors for correspondence: email: stein@binghamton.edu, berrycm@cf.ac.uk

Shortened Title: STEIN ET AL. - JUVENILE PSEUDOSPOROCHNALEAN ROOTING SYSTEM

Keywords: Devonian, Pseudosporochnales, Cladoxylopsida, trees, forests, development

Premise of the Research: Pseudosporochnales (Cladoxylopsida) were conspicuous elements of the Earth's earliest forests. Recent evidence has done much to clarify basic aspects of the pseudosporochnalean architecture, but important questions remain about the developmental processes responsible for growth from juvenile individuals to trees of sometimes considerable size.

Methodology: Presented here is combined compression/permineralization evidence of a young member of the group from a late Devonian (early Frasnian) locality also containing *Eospermatopteris (Wattieza)*, currently the largest reconstructed pseudosporochnalean tree. Standard pyrite preparations were made and analyzed with reflected light.

Pivotal Results: The anatomically preserved portion of the trunk with expanded base lacking a central vascular column shows abundant evidence of appendages with apparent rooting function supplied by traces comprised of primary and often secondary xylem. Traces arise within parenchyma near trunk center and follow lax courses with multiple divisions outward and downward to the surface, finally enveloping the plant base for some distance. In the upper portion of the specimen, likely near the transition between base bearing rooting appendages and aerial shoot, the traces form a vascular plexus toward the periphery of the stem, with the bulk of vascular tissues comprising secondary xylem. Similar but differently oriented vascularization also occurs near the base.

Conclusions: Here we hypothesize a unique form of "bipolar" development in this specimen, and potentially all pseudosporochnaleans, by means of a trunk base bearing an appendicular system of positively geotropic rooting appendages. In addition, we hypothesize that diffuse meristematic activity of the base plus the vascular plexus may have a previously unrecognized role in development of pseudosporochnaleans from the small specimen observed here to large body size. We also suggest that this tissue also offers an explanation for the enigmatic genus *Xenocladia* known from tissue fragments of large size found in coeval marine sediments of New York State, USA. Given current incomplete understanding of development within the Pseudosprochnales, considering the rooting system as "*sui generis*" confers the advantage of adequate description of this organ, without necessarily specifying correspondence or homology with other groups.

Introduction

From their beginnings in the Devonian period, terrestrial forests have been profoundly important to life on Earth, with direct influence on erosion, weathering, mineral cycling, global carbon budget, atmospheric composition and climate (Algeo et al. 2001, Beerling and Berner 2005, Davies et al. 2011, Beerling 2019). In addition, complex interactions between individual trees with other forest elements are fundamentally important to how terrestrial ecosystems develop, maintain themselves, and change over ecological time (Pan et al. 2013). Modern forests comprised of advanced lignophytes (angiosperms and gymnosperms) are familiar to us today, and have an evolutionary history stretching back at least 380 million years (Algeo and Scheckler 1998, Stein et al. 2020). However, from the fossil record we know that the first trees were greatly different from modern ones in overall form, inferred physiology, and mode of reproduction. Nevertheless, certain fundamentals must apply to them, including physical constraints imposed by large size combined with both physiological and developmental means to accomplish growth and maintenance of a large plant body. Modern lignophyte trees largely accomplish this with a structurally dominant secondary body comprised of wood and bark engendered by the vascular cambium and phellogen respectively. This approach may have evolved from a single phylogenetic source related to mid to late Devonian *Archaeopteris* (Meyer-Berthaud et al. 1999), or possibly even earlier among aneurophytaleans (Beck and Wight 1988, Toledo et al. 2018). In our opinion, much of our understanding of what constitutes a tree, and indeed nearly all of currently established terminology relating to development generally, and especially the secondary body (Beck 2010), remains heavily influenced by this single structural strategy. However, there are and have been other successful plants with large body size. In living monocots and cycads, for instance, a typically dominant apex is combined with sustained meristematic thickening via primary or secondary thickening meristems depending upon how these terms are employed in the groups involved (Stevenson 1980, DeMason 1983, Rudall 1991). This produces a substantially enlarged main axis that may continue to increase laterally as development proceeds to accommodate increased structural load and vascular supply required for large size. However, how this form of thickening is related to more familiar secondary development in lignophytes remains uncertain. It

is possible that much of it may have been partially co-opted from ancestral lignophyte developmental processes.

Among non-lignophytes, other useful examples of tree-size plants are known including both ancient and modern tree-ferns (Galtier and Hueber 2001), as well as arboreous isoetalean lycopsids of the Paleozoic (Pigg 1992, 2001, Boyce and DiMichele 2016). In both, we see potentially unique innovations including reorientation of the main plant body from a likely primitive Devonian rhizomatous system to a predominantly upright stance involving an aerial shoot and specialized basal rooting system. The terms "monopolar" and "bipolar" can be applied respectively to these architectures (for instance, Pigg and Rothwell 1979, Sanders et al. 2011), and throughout this paper we enclose these terms in quotes to indicate this meaning. However, problems in terminology immediately develop. Tree-ferns with an upright stance might be better understood as a rhizome in unusual orientation buttressed by a mantle of adventitious roots, and thus fundamentally a "monopolar" system. In stigmarian lycopsids, the rhizomorph consisting of a basal branched rooting axis system bearing appendages (rootlets) provides acquisition functions as well as structural support in what is clearly a "bipolar" architecture as defined above. In this case, the rhizomorph has been termed *sui generis* (i.e., unique) at the organ level (DiMichele et al. 2022). In the Discussion, we offer commentary on this approach including its potential application to the problem described in this report. Clearly, additional functional, developmental or genetic criteria are needed for adequate differentiation between different modes of growth. For instance, "monopolar" and "bipolar" may be further refined to refer specifically to patterns observed early in ontogeny (e.g., Groff and Kaplan 1988, DiMichele et al. 2022 and references therein). In addition, if one wishes to assess several potential levels of homology (Scotland 2010) within or between groups, then phylogeny becomes a crucial aspect of the problem (Rothwell et al. 2014).

Early pseudosporochnalean trees with "bipolar" architecture

The focus of this report is the order Pseudosporochnales (Berry and Stein 2000, Meyer-Berthaud et al. 2007, Durieux et al. 2021, Berry et al. 2022) among the earliest plants in the fossil record to attain large size in what seems to have been an explosive phase in plant evolution (Stein et al. 2012, Berry 2019). Commonly found in Mid to Late Devonian (Eifelian-Frasnian) sediments on remnants of the ancient Euramerican continent in Europe (Berry and Fairon-Demaret 2002, Giesen and Berry 2013), North America (Stein and Hueber 1989, Stein et al. 2007), and northern South America (Berry 2000), the order comprises a discrete subset of taxa within the class Cladoxylopsida. The latter, as traditionally recognized, ranges from late Emsian to Carboniferous age with members identified by their dissected vascular systems (Meyer-Berthaud et al. 2007, Xue et al. 2010). This form of vascular anatomy may include some secondary xylem recognized by radial alignment of tracheids analogous to the situation in lignophytes. Nevertheless, relationships remain uncertain. Both pseudosporochnaleans and cladoxylopsids are currently thought to reside outside the lignophyte clade (Doyle and Donoghue 1986, Toledo et al. 2018), but with unclear relationships both among themselves and potential descendants.

Sharing cladoxylopsid anatomy, the Pseudosporochnales are increasingly well known as entire plants from compressions (Fairon-Demaret and Li 1993, Berry and Fairon-Demaret 1997, Stein et al. 2007, Meyer-Berthaud et al. 2010, Giesen and Berry 2013). Although long the fodder for transformational hypotheses linking primitive plants of the Lower Devonian with more advanced plant architectures (e.g., Zimmermann 1952), recent work has shown that pseudosporochnaleans exhibit a more sophisticated body plan than previously suspected. A main trunk bears lateral branch systems crowded near the apex. The latter functioned in photosynthesis and pteridophytic reproduction much like that of leaves, and were discarded by abscission during further development of the aerial shoot. At the other end, the trunk is typically expanded at the base and bears many undivided or sparsely divided appendages directly on its surface. These are traditionally called "roots" in pseudosporochnaleans indicating their clear functional significance (Dawson 1871, Goldring 1927), although evidence for features often associated with roots in

better known groups (such as root caps, exarch xylem maturation, endogenous development, etc.) remain unknown. In light of this fact, we will employ the admittedly more cumbersome terms "rooting system", "rooting appendage" (or simply "appendage"), or "rooting appendage trace" (for associated vascular tissues), as the case may be, and restricted to pseudosporochnaleans from this point onward in this report. This indicates their interpreted function as distinct from aerial portions of these plants but leaves open possible homology with roots in other groups. We will briefly return to the issue of "roots" in the Discussion. Where known, all pseudosporochnaleans exhibit an upright stance with an extensive rooting system clearly qualifying the plants as "bipolar" in the structural sense defined above. The fossil evidence makes clear that continued longitudinal and lateral growth of the entire plant body in some pseudosporochnaleans was substantial, producing trees of truly impressive height and girth.

The best evidence we have for the pseudosporochnalean body form to date comes from *Lorophyton* and *Pseudosporochnus* at Goé, Belgium (Leclercq and Banks 1962, Fairon-Demaret and Li 1993, Berry and Fairon-Demaret 1997, 2002), from *Eospermatopteris (Wattieza)* at Gilboa and nearby sites in the Catskill region, New York (Berry 2000, Stein et al. 2007, 2021), and from spectacularly intact *Calamophyton* at Lindlar, Rhineland, Germany (Giesen and Berry 2013). The largest of these plants is *Eospermatopteris*, originally described from sandstone casts of a trunk with base as much as 3.6m (12ft) in circumference and rooting system span observed in paleosols of several meters in diameter (Dawson 1871, Goldring 1924,1927). Subsequently, the trunk has been shown to bear crown branches with three dimensionally arranged ultimate appendages of the genus *Wattieza* as originally described from Belgium and Venezuela (Berry 2000). In all, there is no evidence of sustained growth within the branches, and this strongly suggests their ephemeral and modular function. From a nearly complete compression specimen (Stein et al. 2007) the trunk was followed over 6m length from the base 47cm in diameter tapering gently to near the crown at 13cm diameter. In other specimens represented by sandstone casts from Gilboa, the base of *Eospermatopteris* easily exceeds twice that diameter. This strongly indicates some type of lateral development increasing diameter of the main trunk, with continued insertion of rooting appendages

including some at higher levels than possible in smaller individuals (Xu et al. 2017). From paleosol footprints (Stein et al. 2012, 2020, 2021), rooting appendages show no evidence of taper, and are sparsely if at all branched. From this, one might infer regular replacement of older appendages with younger ones again as modular units. However, timing and pattern of their insertion remain unclear.

Pseudosporochnus, found mostly as compressions but with some anatomy of crown branches known, is roughly similar to *Eospermatopteris* in overall form, 10cm in basal diameter and estimated to be 2.5-3m in height, possibly larger. Although differing from *Wattieza* in the organization of crown branches and orientation of sporangia, both genera show scars directly on the trunk as originally described for *Pseudosporochnus* representing abscission of no longer functional branches (Berry & Fairon-Demaret 2002). By contrast, *Calamophyton* has a distinctly different mode of abscission of crown branches commonly leaving 10-20mm of the branch base permanently attached to the trunk. Known complete examples (Giesen and Berry 2013) were apparently smaller than either *Eospermatopteris* or *Pseudosporochnus*, with the tallest specimen ca. 1.5m in height. Multiple specimens of different diameters and heights also strongly support the presence of continued development in *Calamophyton* trunks. In addition, an interesting pattern of decreasing then increasing trunk diameter from stem base toward top was observed, interpreted as epidogenetic primary growth supplemented by acropetal secondary development from the base. The base of *Calamophyton* was also distinctive in consisting of an apparently robust basal disk upon which multiple rooting appendages are attached. Appendage insertion also occurs above the disk, although again the developmental pattern remains uncertain.

Anatomy within Pseudosporochnales has been described for *Calamophyton, Pseudosporochnus* and probably *Eospermatopteris/Wattieza* confirming cladoxylopsid affinity (Leclercq and Lele 1968, Mustafa 1978, Stein and Hueber 1989). In *Pseudosporochnus* and *Eospermatopteris* (represented by *P. hueberi*) this evidence is confined to branches of the crown with traces to ultimate appendages, whereas in *Calamophyton* both branch and stem anatomy are known to some extent. The latter originally termed *Duisbergia mirabilis* reveals a small trunk with a significant amount of secondary xylem (Mustafa 1978).

In other taxa, anatomy of the trunk and base remain largely unexplored, although some anatomically preserved cladoxylopsid material provides intriguing possibilities. In particular for what follows here, highly fragmentary *Xenocladia* from the late Givetian of New York (Arnold 1940,1952) exhibits multiple radially elongate vascular bundles plus internal vascular strands with secondary xylem. This material apparently comprises fragmentary outer portions of a base or trunk of significant diameter. The concept of *Xenocladia* was subsequently expanded to include much more completely preserved material, late Givetian age, from Kazakhstan (Lemoigne and Iurina 1983). However, secondary xylem is now known in several taxa, and given the importance of distinguishing the anatomy of trunk from aerial branches, it seems doubtful that this extension is useful.

Recent work on the anatomically preserved *Pietzschia* has added much to the interpretation of body form in this late Devonian (Famennian) cladoxylopsid (Soria and Meyer-Berthaud 2003, 2004, 2005). The vascular system in *Pietzschia* contains only primary tissues arranged as radially oriented xylem plates with some smaller more elliptical internal vascular bundles. In *P. levis*, the base is preserved showing a primary body consisting of ground, vascular and cortical tissues, surrounded by an extensive mantle of roots with stellate primary xylem. The primary body of the trunk is interpreted to be obconical in form with elaboration of the vascular system and regularization of vascular bundles, suggesting rapid epidogenetic growth at the base, followed by more extended apoxogenetic growth. Total height of *P. levis* was estimated to be ca. 1m (Soria et al. 2001), with upright stance substantially supported by the root mantle in a manner similar to that observed in tree ferns (Soria and Meyer-Berthaud 2004). However, organization of lateral branches in *Pietzschia* differs substantially from known pseudosporochnalean taxa. As a result, the genus is currently considered to be a “non-pseudosporochnalean” taxon within the Cladoxylopsida (Meyer-Berthaud et al. 2007).

Also, potentially applicable to pseudosporochnaleans is anatomically preserved *Xinicaulis* of Late Devonian (Frasnian) age from Xinjiang, China (Xu et al. 2017). Here a silicified trunk is at least 70cm in diameter near its base and contains a system of cauline vascular bundles 50cm in diameter enveloped

within a root mantle up to 10cm thick. Primary xylem of the vascular bundles is enclosed within abundant secondary xylem showing obvious growth increments and a significant thickness of ground tissue and/or phloem. Increase in diameter of the trunk was interpreted to be the result of extensive but diffuse meristematic thickening causing physical rupture of more centrally located cauline xylem strands, and associated with formation of a hollow central area within the trunk. A sizable root mantle consisting of roots of different sizes apparently matches at least to some extent the situation observed in *Pietzschia*. However, this feature does not seem to be indicated for known pseudosporochnaleans, and other important features of the pseudosporochnalean body plan have yet to be demonstrated in *Xinicaulis*. Thus, given uncertainty whether the group actually occurs in China (Berry and Wang 2006), extrapolation of anatomical patterns in *Xinicaulis* to pseudosporochnaleans remains problematic.

Although juvenile examples of *Calamophyton* have been found (Giesen and Berry 2013), possibly the most relevant for this study is *Lorophyton* (Fairon-Demaret and Li 1993). These compressions, 20cm in length, show an expanded base 1.5cm wide with attached rooting appendages (Hetherington et al. 2020). A short and not very wide main stem bears lateral branches we can interpret as being more-or-less equivalent to those in *Pseudosporochnus* or *Wattieza*, although less ramified. From this body form, one can envision a regular pattern of initiation and development to maturity of increasingly complex but ephemeral aerial branches near the crown accompanied by serial senescence of lower branches. Continued lateral development may have provided for increased diameter of the trunk and base, possibly along the lines observed in *Xinicaulis*, associated with sustained rooting appendage initiation.

In the above summary, pseudosporochnalean and possibly related taxa are presented with emphasis on their overall form and possible development to larger size. Although upright and “bipolar” in a functional sense, little is currently known concerning how development proceeds in the plant base to provide supply and support for an increasing aerial system. Presented here is another piece of this puzzle based on pseudosporochnalean material in New York State. From an apparently juvenile plant similar to *Lorophyton* in size and general form, we present anatomical evidence of the crucial basal trunk region

with rooting appendages supplied by appendage traces. From this, we suggest an early developmental stage for interpreting pseudosporchnalean development toward larger size. In addition, we offer a potential interpretation for at least the New York material of enigmatic *Xenocladia*.

Materials & Methods

The specimen described here was collected in 2006 under auspices of the New York State Museum from a quarry on the northwest slope of South Mountain owned by the New York State Department of Environmental Conservation. The quarry exposes sandstone bodies, mudstones, shales, and paleosols typical of the Oneonta Formation, the eastern facies of the Genesee Group latest Givetian to earliest Frasnian in age (Traverse and Schuyler 1994, Sevon and Woodrow 1985, Ver Straeten 2009). The specimen was collected from a sandstone body showing gently dipping foreset beds, possibly representing a small fluvial delta, a few meters distant and at approximately the equivalent level to *Eospermatopteris/Wattieza* described previously (Stein et al. 2007). Macrofloral elements at South Mountain include pseudosporochnaleans, probable aneurophytaleans, and an early *Archaeopteris* (Carluccio et al. 1966, Banks et al. 1985). As such, floral composition is similar to other nearby localities in the Catskill region. Interestingly, however, the site also provides the liverwort *Hepaticites devonicus* (Hueber 1961), plus abundant material of *Serrulacaulis furcatus*, a zosterophyll occurring as a dense mat (Hueber and Banks 1979).

As originally found, a single surface impression of an individual with pseudosporochnalean body form was observed (fig. 1*A*) plus poorly preserved fragments that may represent detached branches (fig. 1*B*). The counterpart was missing, except for small pieces unfortunately of limited value. The impression was cut from the exposed surface by diamond saw and collected as a ca. 0.75x1.0m block. Images of the surface were made in the field and lab using a digital camera in incident and polarized light.

In addition, a pyrite (iron disulphide) nodule spanning the width of trunk base, and fitting precisely within the impression, was collected (figs. 1*C,* 2*A* a). This was embedded in Ward's Bioplastic (Ward's Natural

Science Company, Henrietta NY, USA) and cut into transverse wafers (#3-18) at 2 mm intervals, with end blocks (#1-2) representing the apical end of the nodule (fig. 2*B*). The apical end block (#1) was subsequently cut into transverse wafers (#2C-6C) at 2mm intervals and conserved, but unfortunately yielded little useful information. The basal end block was cut longitudinally normal to bedding plane approximately midway through the nodule (fig. 2*B*), with one half continuing the series of transverse wafers at 2mm intervals to the nodule base (#19R-24R), and the other half cut into longitudinal sections with wafers at 2mm intervals from the center of the nodule outwards (#1L-7L). Following an established method (Stein et al. 1982), all wafers were re-embedded in Ward's Bioplastic to stabilize pyrite surfaces. Most were then fine-polished and etched with nitric acid. After etching, wafers were treated with ammonium hydroxide to neutralize the nitric acid, re-acidified in hydrochloric acid, and then dehydrated with a progressive ethyl alcohol series to xylene, prior to making permanent mounts using Eukitt (Electron Microscopy Sciences, Hatfield PA, USA). Images of all pyrite wafer surfaces were made under diffused incident light from multiple sources, using a Leitz Ortholux microscope and attached digital camera.

To facilitate mapping of anatomical features, *camera lucida* drawings of both surfaces of each wafer were made using a Wild M5 binocular microscope. In addition, high resolution stitched images of each surface were made from 16-100 individual photos each, and verified by visual observation. A summary of this information is provided here (figs. 3-4), with one surface of each wafer reversed horizontally to provide a consistent perspective. In these, some rooting appendages traces followed between wafer surfaces are indicated by colored markers. *Camera lucida* drawings and high-resolution stitched images are deposited along with the specimen (comprising both impression and permineralized preparations) at the New York State Museum, Albany, NY (NYSM 19,312). More detailed versions of these figures, plus images of each section surface, may also be found online (Stein et al. 2022).

Results

The plant, preserved primarily as a surface impression but also with occasional carbon flecks and some limonite surface coating, consists of a single individual with expanded base 50-60mm in diameter, and trunk 31mm in diameter preserved in organic connection for a length of 290mm (fig. 1*A*, 2*A*). The base shows attachment of multiple rooting appendages, with up to 12 counted on the surface but probably many more both above and below bedding plane. All appendages are more-or-less of equal in size with diameters 8-9mm, and showing little evidence of taper. They appear to arise at more than one level near the trunk base, mostly if not entirely confined to the region of expanded diameter (figs. 1*A*, 2*A* a). This region shows longitudinal striations at ca. 1 mm scale and corresponds to similar patterns on the pyrite nodule containing anatomy (figs. 1*A* arrow a, 2*A* a). Free rooting appendage impressions on the specimen surface extend to lengths of at least 120mm from the base with individual appendages clearly incomplete. Their surface texture is smooth, and some show central longitudinal grooves presumably representing vascular tissue. Above the level of rooting appendages (fig. 2*A* b) the trunk has smooth surface texture with distinct longitudinal ridges and furrows apparently associated with the insertion of at least 4-5 lateral branches over its preserved length (figs. 1*A* arrows, 2*A* triangles). The branches are clearly staggered, but exact organotaxis of the branches cannot be determined due to limited material. In each instance, the branches are 6-6.5mm in width near their base, and appear to be broken at or near insertion on the trunk.

Above the recognizable trunk, the collected slab and isolated counterparts show faint impressions of closely associated smaller branch systems, but these are poorly preserved and not attached. An example of one of these (fig. 1*B*) shows a central axis 10mm in diameter apparently bearing numerous lateral appendages with at least their basal portions preserved. Unfortunately, little can be determined about the exact form or arrangement of these laterals.

General anatomical features

The pyrite permineralization shows ground tissues and the dissected vascular system of this small individual (figs. 3-5). Based on both position of the nodule in the impression and from anatomical

features described in detail below, preserved tissues span a region from the base of the plant upwards in the trunk toward the aerial main shoot. We state at the outset here that nearly all anatomically preserved vascular bundles will be interpreted in this report as rooting appendage traces – here recognized by the presence of xylem or associated tissues that diverge outward and downward, likely supplying the rooting appendages observed in close association on the compression. We recognize that this interpretation may be at variance with more typical interpretations of cladoxylopsid anatomy, but will defer this issue to the Discussion. However, to further orient the reader, the entire system of rooting appendage traces in this specimen bears a resemblance to leaf traces in appendicular systems as in seed plants, although of course no homology is implied and divergence directions of the traces are inverted. Because of this unusual context we use **acropetal** (upwards toward the shoot apex) versus **basipetal** (downwards toward the trunk base and beyond) as orientation indicators for the plant as a whole, as is customary. In addition, and possibly somewhat at variance from common usage, we use **proximal** to indicate more acropetally and centrally located appendage traces, versus **distal** for more basipetal and/or peripherally located appendage traces as the case may be. Note that these terms are only meant as static positional descriptors.

Overall, transverse dimensions of the pyrite nodule range from 11mm acropetally at widest dimension parallel to bedding expanding to 32mm toward the base (fig. 5*F*-*G*). Although the out-of-round dimensions at all levels are likely due to compression normal to bedding, expansion of the permineralization basipetally is unquestionably a feature of the expanded base of the trunk, also observed in the accompanying impression (figs. *1A,C*, 3-4, 5*A*-*C*). In transverse section, the center portion of the stem base appears more-or-less complete except for zones comprising carbonized wings parallel to bedding plane. In acropetal regions, there is better representation of the vascular system on one side of the specimen (i.e., toward the top in fig. 5*A*). The outer ground tissue generally consists of an aerenchyma including extensive intercellular spaces (fig. 5*B* arrows a), with more central ground tissue comprised of cells crushed normal to bedding (fig. 5*B* arrows b). In basal portions of the trunk observed in both transverse and longitudinal views (figs. 4, 5*H*-*K*), a similar zonation of ground tissue is found,

307 although disrupted to a greater degree by amorphous pyrite surrounding vascular tissue, as described
308 below. Cortex and epidermis are not observed.

309 ***Organization of the vascular system***

310 In the acropetal region of the pyrite nodule (figs. 3 *sections 3b-8b*, 5*A*), radially elongate single, U or Y
311 shaped vascular bundles are observed containing relatively abundant secondary xylem for this specimen
312 (ca. 8-20 tracheids in radial rows) in a zone toward the periphery (figs. 5*A*, *6A-C*). This zone is
313 incomplete but based on the distribution of other parts of the vascular system probably comprised a nearly
314 full ring of elongate strands. Despite this appearance, however, we observe that the outer vascular
315 bundles in this specimen are instead almost entirely composed of closely associated rooting appendage
316 traces that can be definitively traced through a series of transverse sections in the basipetal direction.
317 Given the unusual context of this vascular tissue involving rooting appendages, which we believe to be
318 important as discussed below, we term the entire association of vascular bundles at this level and
319 elsewhere the **vascular plexus** in order to distinguish it by name from potentially similar-looking tissues
320 in other contexts. As shown in detail below, individual rooting appendage traces distally separate from
321 others of the vascular plexus, and diverge basipetally to the permineralization surface. Beyond this,
322 attached continuations of individual appendage traces persist on the permineralization surface for some
323 distance in the basipetal direction. These appear as partially preserved arcuate bands typically filled with
324 crushed organic contents (fig. 6*F* arrow b). Further down, similar arcuate bands on the surface of the
325 permineralization are observed throughout its entire length to the base and in many cases are also clearly
326 associated with proximal rooting appendage traces located more centrally within the trunk's interior. All
327 of these bands are interpreted as partial appendage compressions enveloping the trunk's outer surface, and
328 responsible for the pattern of external grooves and ridges observed on the pyrite nodule before sectioning
329 (fig. 5*F-G*). These in turn match in size and position the longitudinal surface patterning observed in the
330 corresponding region of the impression (fig. 1*A* arrow a), closely associated with rooting appendage
331 impressions. However, one-for-one correspondence of the arcuate bands on the permineralization with

rooting appendage impressions, although likely, was not observed due to the fact that sections of the pyrite nodule were made prior to this interpretation.

More centrally in the permineralization, there are additional vascular bundles that are observed to merge basipetally with inner portions of the vascular plexus. However, these also prove to be rooting appendage traces that further down also separate and diverge to the permineralization surface becoming apparent appendage compressions. Proceeding toward the mid-region and base of the permineralization (fig. 3 *sections 8f-18f*, 5*B-D*, 7*A-D*), peripherally elongate strands of the vascular plexus diminish in length with individual appendage traces separating into individual vascular strands. These together comprise several complete or partial imbricate cones of rooting appendage traces that successively expand to the periphery in the basipetal direction.

Toward the basal end of the nodule, longitudinal sections confirm distal trajectories of rooting appendage traces from center outward and downward in a cone-like pattern expanding basipetally, apparently with division of some traces into multiple vascular strands (figs. 4, 5*H-K*). At the extreme basal end of the nodule, traces are enclosed within extensive amorphous pyrite. This may represent the vascular system plus some enveloping tissues descending away from the base of the trunk in transverse (fig. 5*E* arrow, 10*D*) or oblique (fig. 5*J* arrows, 5*K* arrow, 10*C*) views. Although poorly preserved, these seemingly correspond to rooting appendages proceeding from the base of the trunk observed on the impression (figs. 1*A*, 2*A*).

Rooting appendage trace initiation from the outer surface of the vascular plexus

Looking at the apical (i.e., most acropetal) preserved region in greater detail, production of appendage traces at the periphery of the vascular plexus appears evident. Here, the tips of some primary xylem ribs, partly preserved in limonite and appearing lighter in tone in the photographs, are greatly enlarged by extensive secondary xylem (fig. 6*B* arrows a). In addition, a rooting appendage trace is present within what appear to be its own surrounding tissues, although this is incompletely preserved (fig. 6*C* arrow b).

Shown in detail from successive wafer surfaces, separation of this appendage trace occurs in a more-or-less radial plane (fig. 6*D* arrow b). The immediately adjacent basipetal wafer surface (fig. 6*E* arrow b) shows abrupt reorientation of tracheary elements longitudinally, with the detached appendage trace now in transverse section. Unfortunately, configuration of the primary xylem is unclear, but conspicuous secondary xylem is apparent along with adjacent ground tissues suggestive of cortical tissues of the rooting appendage itself. This appendage can then be followed basipetally for a couple of wafer surfaces and ends as an arcuate compression interpreted to be the remnant of the appendage on the pyrite surface (fig. 6*F* arrow b). Thus, available evidence indicates rooting appendage separation from the exterior of the vascular plexus at this apical level. Although not definitive, the angle of departure with abrupt distal change in orientation is different from appendage trace patterns observed elsewhere and may suggest production of some rooting appendages in a different manner.

Rooting appendage traces within the vascular plexus

Looking at more internal portions of the vascular plexus, it is evident that rooting appendage traces within, whether part of radially directed xylem ribs or as separate xylem bundles, can be identified and followed basipetally (fig. 6*A-C* arrows c-d). At distal levels all ultimately separate into individual traces and depart as partial rooting appendage compressions on the surface of the nodule ca. 1/3 of the way from acropetal end to the base (fig. 3 *sections 3f-8b*, 6*A-C*). Further inside at apical levels in the specimen are additional appendage traces, consisting of both primary and secondary xylem, that proceeding basally join with the vascular plexus. At different levels these appear as separate elliptical vascular bundles or part of elongate primary xylem ribs (fig. 6*A-C* arrows e-h). Distal fusion of the bundles with the inner surface of primary xylem ribs is observed, as well as lateral fusions of adjacent ribs (figs. 6*A-C* arrows f, 7*A-D* arrows f). It must be noted, however, that whether apparently fused to other xylem elements or not, component appendage traces can still be recognized by presence of primary xylem and by position. Proceeding in the basal direction, all traces ultimately separate from each other and migrate to the surface in lax fashion (in contrast to the more abrupt radial departure of acropetal traces described above),

occasionally subdivide, and depart distally as peripheral arcuate rooting appendage compressions on the surface ca. mid-length on the nodule (figs. 3 *sections 3f-12b*, 7*D*). Thus, with the possible exception of the most peripheral portions of radially oriented xylem ribs that could not be followed acropetally due to incomplete preservation, the entire vascular plexus consisting of radially elongate xylem ribs apparently comprises closely associated rooting appendage traces. These traces become incorporated into ribs at some levels and sometimes show apparent primary xylem continuity with other portions of a xylem rib (figs. 6*A* arrow g, 7*B* arrows e, i, 10*A*). Over the full series of wafer surfaces following a particular trace, however, this appearance is clearly localized. In many other cases, the primary xylem of each appendage trace remains separately identifiable although situated within a xylem rib or other parts of the plexus and enclosed by secondary xylem.

Radially directed xylem ribs within the vascular plexus measure 4.5 mm in their maximum observed radial extent (fig. 5*A*), and 0.6 mm in width, but widening considerably toward the periphery to as much as 1.7 mm. Rooting appendage traces when separate are typically 0.7 mm or less in diameter, and variable in size mostly due to the amount of secondary xylem present at any particular level. Based on observation of appendage traces followed in total, including those specifically identified above, it appears that many if not all occur within the vascular plexus in recognizable radial zones, (fig. 6 arrows a-b, c-d, e-h), resulting in an imbricate pattern of widening divergence in the basipetal direction to the surface (fig. 3 *sections 3f-6f*, *sections 3f-8b*, *sections 3f-12b* respectively).

More internal rooting appendage traces

Further toward the center of the trunk at apical levels are additional vascular bundles 0.2 mm or less in diameter, with obviously lesser amounts of secondary xylem (fig. 6*A-C* arrows i-k). These bundles follow a similar pattern of widening basipetal divergence (figs. 7*A-D*, 8*A*) as appendage traces (fig. 3 *3f-15f*), supplying yet more rooting appendage compressions on the nodule surface ca. 2/3 of the way from tip to base. Due to their location in the specimen, preservation is sufficiently complete at some levels to allow recognition of an extensive set of traces comprising partial arcs to a near complete whorl of traces

(figs. 3 *7f-9f*, 7*A* arrows j, k, ★). The course of one rooting appendage trace of this set is figured in more detail here (figs. 6-8 all arrows k). In this instance, following the trace toward the base it first dichotomizes (figs. 6*B-C*, 7*A-B*, *E-G*), followed distally by apparent fusion with outer appendage traces due to envelopment by secondary xylem (fig. 7*D,H*), and ultimate departure as rooting appendage compressions at the surface (fig. 8*A*).

Following from midway in the permineralization to the base, at least three additional imbricate sets of vascular bundles comprising partial arcs or complete whorls of rooting appendage traces are recognized. These can be followed for some distances (figs. 3-4 *sections 6f-17f*, *sections 15b-21Rb*, *sections 19Rf-24Rb*) and also show lax distal departure with each set of traces in cones expanding toward the base. All traces diverge to the surface basipetally and continue as arcuate compressions (fig. 8*A-D* arrows l-o) or in the basal levels of the permineralization as possible poorly preserved complete rooting appendages in transverse to oblique section (fig. 5*E,K* arrows).

At ca. ⅓-½ distance from apical to basal end in the specimen (fig. 8*A-D*) the vascular plexus observed acropetally has become modified to the extent that radially elongate ribs are no longer apparent in this region. In addition, the diameter of the trunk has expanded considerably indicating that observations are clearly within the bulbous base of the trunk as observed in both impression and permineralized nodule. With this, the geometry of the vascular system, especially the relationship of rooting appendage traces to surface of the trunk, also seems to be different. Most notably in the more acropetal of the three imbricate cones of traces mentioned above (fig. 8*A-D* arrows l-n) appendage traces are recognized proximately as small circular to elliptical strands. These show distal dichotomies in the manner described above. However, approximately midway from trunk center to the periphery groups of rooting appendage traces become enveloped in significant amounts of secondary xylem, although still allowing for their separate identification (fig. 8*E-F*, 9*A*). This occurrence is potentially comparable with the vascular plexus association of strands observed acropetally, although here the traces are greatly reduced in amount of fusion and the possible equivalents to xylem ribs are now oriented parallel to the trunk surface (fig. 8*B*

arrows l-m, *E-F* arrows l). Nevertheless, primary and secondary xylem tracheids remain oriented longitudinally. Beyond this level moving toward the base, appendage traces with secondary xylem again separate into individual strands with most showing additional dichotomies (fig. 8*C-D* arrows l-n, 9*A-D* arrows n), possibly more numerous here than observed acropetally. In one instance, an appendage trace division is observed in which one of the resultant traces is oblique and reaches the trunk surface considerably above the others (fig. 9*B* right most arrow n).

The remaining two arcs to whorls of rooting appendage traces comprising widening cones basipetally (figs. 3-4 *sections 15b-21Rb*, *sections 19Rf-24Rb*) follow much the same pattern of origination nearer the expanded trunk base center, bifurcations, and divergence to the outer surface base as described above. The basal-most set is observed in both transverse and longitudinal sections (fig. 5*D-E*, *H-K*) confirming the lax nature of appendage trace divergence. Only one example is illustrated in detail here (figs. 8*B-D* arrows o, 9*E-I* arrows o). At the basal end of the permineralization representing the trunk base, rooting appendage traces are observed in oblique to transverse views (figs. 5*J-K* arrows, 10*C-D*) in addition to arcuate compressions along lateral surfaces. Remnants of the xylem occur within apparently individualized appendages (fig. 10*D*), but with uncertain configuration due to poor preservation.

Histological details and developmental interpretations

For the sake of brevity, the following paragraph pairs consist of additional observations followed immediately by interpretations especially as both may relate to the developmental perspective we present below. We acknowledge that other interpretations remain possible.

In transverse section, the primary xylem of rooting appendage traces consists of variable numbers of tracheids with the smallest cells located toward the center (fig. 7*E-F*, 8*E-F*, 10*B*). All tracheids are quite small ranging between 17-30µm in transverse view, with protoxylem versus metaxylem not distinguished in either transverse or longitudinal sections. In several instances, appendage traces are observed to divide

once to several times as they follow an outward course basipetally over considerable longitudinal distance without noticeable disruption of adjacent tissues.

Interpretation: This suggests development of the strands in a manner more-or-less similar to appendicular appendages in lignophytes, but in the basipetal direction. This apparently contrasts with endogenous initiation of roots seen in modern examples, typically involving noticeable disruption of primary tissues. However, two examples of appendage trace initiation mentioned above (e.g., fig. 10*C-D*) may be exceptions to the general pattern.

As described above, several rooting appendage traces within the acropetal region of the specimen can be followed from more internal parts of the permineralization into the vascular plexus, with individuality of individual traces recognizable (figs. 6*A-C*, 7*A-D*). However, within radially elongate bundles in this region, primary xylem sometimes appears to comprise more-or-less continuous bands running along midplanes of the ribs (fig. 10*A*). Close inspection, however, shows that these tracheids are flattened normal to these midplanes. Other vascular bundles often contain more than one loosely defined center of organization comprised of primary xylem (fig. 10*B*, arrows), with multiple appendage traces giving the bundle an elongate appearance.

Interpretation: Thus, despite uncertainty about the peripheral-most portions of some xylem bundles of the vascular plexus in the acropetal portion of the specimen, existence of primary xylem of a main stem other than rooting appendage traces is not to be supported by current evidence. Instead, the elongate bundle appearance comprised of multiple appendage traces of the vascular plexus seems largely a function of more extensive secondary xylem development sometimes causing compression of the primary xylem.

In most regions of the specimen, the boundary between primary and secondary xylem is indistinct often containing larger cells as much as 45μm in transverse diameter. Secondary xylem proceeds peripherally as a compact tissue of thick-walled tracheids in radial files (figs. 7*G-H*, 8*E-G*, 10*A-B*). Tracheid diameters are 20-40μm in tangential dimension relative to the vascular bundle, but vary in size related to

augmentation of radial files due to apparent tangential divisions. Diminishment of the radial dimension of tracheids near the outer boundary of the secondary xylem is also commonly observed (fig. *10A-B*). In many cases the outer boundary of the secondary xylem appears irregular with some separation of tracheid files toward the bundle periphery, as well as faint indications of files of small cells continuing into surrounding amorphous pyrite (fig. 10*A-C*).

Interpretation: It is possible that the secondary xylem especially near the periphery of this tissue reflects the presence of thinner-walled cells serving a function analogous to ray parenchyma in lignophytes. However, definitive evidence for a thin-walled cells within well-preserved secondary xylem is not observed.

Although a generally compact tissue in transverse section at most levels in the permineralization, longitudinal and very likely oblique views of secondary xylem of rooting appendage traces near the base of the trunk provide a somewhat different view. Here secondary xylem tracheids occur in radial files but appear much more variable and often larger in diameter. In addition, these cells sometimes contrast sharply with the primary xylem in orientation (fig. 10*C,E*). In these circumstances, it remains unclear whether the secondary xylem tracheids are in fact elongate or instead much shorter. Bordered pitting is observed in primary and secondary xylem in both transverse and longitudinal tracheid orientations (fig. 10*E*). Pits are circular to transversely elongate with elliptical apertures, and uniseriate to multiseriate on wall faces depending on the size of tracheid observed. Protoxylem wall thickenings are not observed.

Interpretation: Unusually shaped tracheids in the basal region are possibly organized to perform a function analogous to transfusion tissue (Beck 2010). This in turn may relate to a difference in function - structural support and longitudinal transport in regions of well-formed vascular plexus in more acropetal regions versus absorptive functions of rooting appendage xylem closer to the trunk basal surface.

Surrounding the secondary xylem throughout the permineralization is a mostly amorphous band comprised of crystalline pyrite and organic cell fragments, suggesting lack of preservation of primary or

secondary phloem, and possibly also some physical separation between appendage traces or entire rooting appendages within surrounding tissues. In acropetal regions of the specimen associated with composite radial bundles of the vascular plexus, amorphous regions are narrow, 0.02-0.3mm wide (fig. 10*A-B*). In basal parts of the specimen, the amorphous pyrite regions surrounding appendage trace xylem are greatly expanded (fig. 10*C-D*).

Interpretation: The continuation of cell fragments in rows from secondary xylem into these regions suggests presence of secondary phloem, at least in part, although evidence for a bifacial vascular cambium is not observed. Basal expansion of amorphous regions may in fact represent entire rooting appendages within, or departing from, the base of the trunk. Lack of preservation of tissues surrounding the xylem in these regions may suggest thin-walled cells of low preservation potential, or that rooting appendages were in part hollow. The large regions of amorphous pyrite might also suggest possible disruption of ground/cortical tissues in this region due to a more endogenous-style development of entire rooting appendages.

Several rooting appendage traces were followed in the proximal and acropetal direction toward the center of the trunk base as far as possible. In one example shown here (fig. 11*A-E*), typical of the situation encountered, secondary xylem typically diminishes to the point where only primary xylem remains (fig. 11*A-C* arrows). Beyond that, primary xylem becomes indistinguishable (fig. 11*D-E* arrows), although in several instances the amorphous zone surrounding known traces remains recognizable for a further distance acropetally. In no instance in the specimen is there any evidence of a central vascular system in the trunk base to which individual appendage traces connect.

Interpretation: The conclusion we reach is that tracheid wall maturation ceases proximally in the rooting appendage traces. If true, then it may be hypothesized, admittedly with scant evidence, that the amorphous zones shown to be in continuity with appendage traces acropetally represents locations of provascular tissue that end blindly within the non-vascular center of the specimen.

Ground tissue aerenchyma especially in the better-preserved peripheral zone noted above (fig. 5*B* arrows a) exhibits a conspicuous gradient following this tissue from apical regions of the permineralization toward the base (fig. 11*F-H*). At acropetal levels, the aerenchyma consists of isodiametric cells with rounded or angular profiles, 35-100µm in transverse diameter, organized in a loose arrangement including irregularly shaped intercellular spaces (fig. 11*F*). Cell walls are relatively thick, with thinner walls observed close to vascular bundles and toward the center of the trunk. Proceeding toward the base of the specimen, cell wall thicknesses decrease and compactness of the tissue increases, as observed in both transverse and longitudinal views (fig. 11*G-H*). In addition, cell contours typically become much more irregular in shape.

Interpretation: In longitudinal section in the basal region of the specimen (figs. *5I-K*, 11*H*), there is little evidence of organization, such as cells in longitudinal files, as might normally be expected of a primary body derived from a discrete apical meristem. Instead, disorder in this tissue with cell walls suggesting less structural integrity indicates to us the presence of substantial proliferation of tissue produced by diffuse meristematic activity in the ground tissue regions cutting off cells in multiple directions. Although not restricted to a readily apparent meristematic zone, we suspect that the expanded diameter of the trunk base of the plant is related to this form of meristematic activity.

Discussion

Although the compression portion of the specimen described here is incomplete, sufficient evidence exists for a main axis or trunk, an expanded base with attached rooting appendages, and an aerial portion bearing bases of lateral branches. This matches architecture previously observed in the Pseudosporochnales and combined with apparent cladoxylopsid anatomy we think this allows reasonably confident assignment to the group. Moreover, placement of this individual with *Eospermatopteris* (*Wattieza*), *Pseudosporochnus* and *Lorophyton* within the Pseudosporochnales appears more likely, as opposed to *Calamophyton* – the later having abscission of branches leaving discrete stubs on the stem and "an apparently flattened basal disk" (Giesen and Berry 2013). Although the overall size of the new plant

551 is somewhat larger than *Lorophyton*, in our opinion the two together provide compelling complementary
552 views of a likely early stage in development of tree form within the group.

553 The unique contribution this specimen provides is cellular preservation of the trunk base showing
554 preserved cellular features including mode of production of its rooting system. At this apparent stage in
555 development, there seems to be little support for the presence of an extensive "root mantle", nor is there
556 evidence for obconical growth of the primary body. Instead, a "bipolar" organization for this plant is
557 indicated, potentially applicable to all pseudosporochnaleans, consisting of a basal expanded trunk
558 showing rooting appendage trace initiation in the basipetal direction, an aerial shoot with lateral branch
559 production acropetally, and a shoot to base transition zone between them. As employed here, the term
560 "bipolar" is intended to suggest probable organization of pseudosporochnaleans as having a juvenile
561 upright stance with no sign of an earlier developmental stage involving the rhizomatous habit. Of course,
562 it remains entirely possible that such a "monopodial" stage may have existed. However, preserved tissues
563 in our specimen provides no evidence for this, nor is there evidence of any kind within
564 pseudosporochnaleans to support such a view. Thus, given the current state of our knowledge it seems
565 parsimonious to postulate that what we observe is fundamental to pseudosprochnalean architecture,
566 especially as it relates to attainment of large size from significantly smaller individuals. In addition, the
567 rooting system described here appears unique in organization among known Devonian plant groups.

568 ***Pseudosporochnalean rooting system as* sui generis *organ?***

569 As mentioned in the Introduction, DiMichele et al. (2022) offered a similar "*sui generis*" (= unique)
570 proposal to cover the rhizomorph rooting organ of stigmarian isoetaleans. From our reading, they based
571 their argument on two claims: (1) single origin of rhizomorph rooting function within lycopsids based
572 upon current understanding of phylogeny, and (2) branching at an early stage in sporophyte
573 embryogenesis allowing identification of the rhizomorph as a separate plant organ. The second claim
574 certainly lies within botanical tradition where early developmental features, especially embryos enclosed
575 within seeds of seed plants, are often viewed as significant in determining polar orientation and basic

576 organography. However, with the increasing recognition that developmental pathways often occur as
577 functional modules in different developmental contexts, simply referring to temporal order in an
578 individual's ontogeny may not be all that reliable. Moreover, recognizing that many developmental
579 pathways likely predate the plant groups and developmental contexts in which they are observed (i.e.,
580 "deep homology" in Shubin et al. 1997), this further complicates assessment of fundamental
581 organography. (We note that DiMichele et al. give an example of this when citing similarities in gene
582 expression between stigmarian rootlets and roots outside this group thereby suggesting a fundamental
583 difference between leaves and rootlets within stigmarians). So, how should the *sui generis* formulation be
584 interpreted? We suggest that it is informed conjecture based upon available evidence, nothing more, but
585 certainly nothing less. As a result, it seems that other conjectures (such as the rhizomorph being the first
586 division of the embryonic axis as previously proposed by Rothwell et al. 2014 based on similar evidence)
587 might also be viable and have some weight. Thus, until issues of developmental process are more fully
588 worked out, it might not be possible to reliably decide between rival claims of this type. It may turn out
589 that the answer for stigmarians will be a mixture of the two ideas, and similar results may apply to other
590 groups as well.

591 So, are the different conjectures useful? Here we see an important difference. Whereas the earlier claim
592 carries with it the hypothesis of direct correspondence and potential homology between components of
593 the aerial shoot and rhizomorph, DiMichele et al.'s assertion of *sui generis* does not, or at least not
594 necessarily. While acknowledging that the aerial shoot and rhizomorph in these plants likely share
595 underlying genetics and some developmental processes, focus is squarely placed on observed rhizomorph
596 features and evolutionary patterns within the "*sui generis*" organ itself.

597 Applying the *sui generis* concept to the juvenile pseudosporochnalean entire rooting organ described here,
598 and parsimoniously interpreted, similarly allows direct analysis of this organ without having to
599 incorporate prior expectations based upon supposed correspondence or homology outside, or even inside,
600 this group. We recommend doing this as an interim measure until relevant developmental and

601 comparative data become more complete. Nevertheless, we acknowledge that application of this concept
602 to pseudosporochnaleans is quite different from that in stigmarians. Obviously, the evidence base for
603 pseudosporochnaleans is far less extensive, and as a result our understanding of phylogeny is less secure.
604 Added to this is current uncertainty about the appropriate circumscription of pseudosporochnalean taxa
605 (such as including or excluding *Calamophyton* and potentially other cladoxylopsid taxa) to which this *sui*
606 *generis* concept should be applied.

607 However, given a *sui generis* interpretation for the rooting system of pseudosporochnaleans, what
608 consequences might this entail? For one, this approach permits consideration of tissue and organ
609 organization, such as here with vascular plexus and rooting appendage, specifically within the unique
610 context of the pseudosporochnalean rooting system, without becoming entangled in phylogenetic and
611 terminological difficulties involving comparisons with other groups. To be clear, such comparisons are
612 important. However, given our current knowledge this is clearly premature, and the best thing we can do
613 is state the more limited context in which our terms are employed. Future comparisons may ultimately
614 reveal, for instance, that the vascular plexus as defined above should be interpreted in a more
615 comprehensive way. Likewise, the term "root" as traditionally employed within pseudosporochnaleans
616 may be given a satisfactory reinterpretation in line with roots observed in later plant groups.

617 ***What about "roots"?***

618 In the review process, we have been advised to adopt the term "rooting appendages" as opposed to the
619 more traditional "roots" for pseudosporochnalean structures that can be reasonably interpreted as
620 exhibiting rooting function. This function may be inferred from their position within the
621 pseudosporochnalean "bipolar" body plan combined with existing evidence that these appendages occur
622 within entire rooting systems preserved in paleosols (Stein et al. 2012, 2020, 2021). The intent, of course,
623 is to avoid conflation of rooting function with the anatomical or developmental features in better-known
624 plants, such as especially represented by extant dicot angiosperms. Certainly, this distinction needs to be
625 made since failure to do so engenders two related fallacies: 1) assuming that pseudosporochnalean rooting

appendages actually exhibit some or all features homologous with modern roots, and 2) requiring that the fossil record of rooting appendages in pseudosporochnaleans, not to mention other Devonian fossil groups, must necessarily show some or all of these features to satisfy interpretation of their rooting function. Regarding the first, beyond anatomical material presented in this report all of what we know within pseudosporochnaleans is based on compression evidence. This includes attached rooting appendages to bases in several instances (*Lorophyton*, *Eospermatopteris*, *Calamophyton*). Combining this with anatomically preserved roots showing stellate and exarch protosteles within root mantles in *Pietzschia* and *Xinicaulis* might supply a composite picture. In both, however, we caution that there are observed differences in anatomy between root traces within the trunk base versus stelar architecture of independent roots in these potentially related taxa. As a result, comparison with the "appendage traces" described in this report remains uncertain.

Regarding the second fallacy mentioned above, it is clear that much remains to be resolved in assessing phylogeny, especially involving features often associated with roots within seed plants, other lignophytes, and fossil or living non-lignophytes. In our opinion, it seems highly unlikely that root caps, exarch primary xylem, and endogenous development in extant plants all originated as a single innovation. Thus, it is clear that the phylogeny of plants exhibiting some or all of these features needs to be more fully worked out before any can reasonably be applied as evidential prerequisites for remote Devonian groups. In fact, these fossil groups may end up playing a pivotal part in unravelling the actual pattern of acquisition of these features (Hetherington & Dolan 2018, Hetherington et al. 2020). In our opinion, however, much work remains to be done especially in formulating cladistic characters that have a defensible developmental basis. On the other hand, and respecting *sui generis*, it may turn out that rooting appendages with traces forming a vascular plexus within pseudosporochnaleans was a unique innovation restricted to this group. We need to allow for this possibility as well.

So, for the sake of clarity what terminology should researchers employ for rooting structures especially within problematic Devonian groups? Here we make a modest suggestion recognizing different

651 approaches may also be valid. Perhaps, it might be best to restrict the term "root" to refer explicitly to
652 rooting function as is at least one of its traditional meanings. Within pseudosporochnaleans, "rooting
653 appendage" then becomes "root" and we must be careful to distinguish trunk "base" from "root" in this
654 functional sense. However, when treating comparisons within or across groups it also seems useful to
655 give the rooting system's inferred phylogenetic context as in "pseudosporochnalean root" or "lignophyte
656 root", as the case may be. In addition, unique terminology might also be employed in specific cases as in
657 "rhizomorph" and "rootlet" as currently restricted to rhizomorphic lycopsids. Furthermore, we can
658 readily see useful extension of this approach to other features that often provide terminological confusion,
659 such as with "pseudosporochnalean secondary xylem" or "lignophyte secondary xylem" (Stein 1987).

660 ***Visualizing pseudosporochnalean architecture***

661 An important consequence of adopting *sui generis* as an interim stance, is the freedom to develop
662 hypotheses of complete-plant development specifically tailored to pseudosporochnaleans that are
663 conspicuously at risk of being overturned by further evidence. To do this, we suggest some ideas in this
664 and the following sections employing a "strong inference" approach (Platt 1964, see also Stein and
665 Hueber 1989 for a specific example within pseudosporochnaleans). This necessarily involves visualizing
666 associations or processes that reach beyond demonstration with currently available evidence, and stands
667 in stark contrast to adopting a non-committal perspective and terminology that may confer a sense of
668 safety but says little.

669 Independently derived rooting systems as seen in seed plants and stigmarians are typically organized
670 around a well-defined apical meristem functioning in positive geotropic orientation. The activity of these
671 meristems is often recognizable in mature tissues, especially in angiosperm roots, by the longitudinal
672 columns of cells produced by serial cell divisions near the apex. In young pseudosporochnaleans, as
673 indicated by this specimen however, it seems that growth may not have functioned in this way. Instead,
674 cells with fewer intercellular spaces and thinner cell walls toward the basal portion of the trunk suggests
675 less maturity of tissues in that direction. Multiple shapes and evident lack of organization of cells in these

tissues leads us to suspect the presence of meristematic thickening, but not in well-defined meristematic zones or regions. In addition, a well-defined primary body consisting of a central vascular column and mature cortical tissues seen in other groups also seems to be absent. Instead, rooting appendage traces in successive partial arcs or full whorls become apparent near the center of the trunk and follow lax imbricate courses through aerenchymatous tissue basipetally (fig. 12). The whole pattern of rooting appendage production is thus highly suggestive of a positively geotropic body with appendicular appendage development. If true, then xylem maturation within rooting appendage traces may have proceeded from the surface toward the inside of the trunk perhaps in a way similar to that seen in seed plant aerial appendicular systems. From all this, it is possible to imagine continued meristematic behavior within the basal region of the plant contributing to indefinite increase in size of the trunk base as well as continued rooting appendage initiation (see below).

At the other end of the preserved specimen, at a level closer to the aerial stem of the plant, other features of our specimen may be informative. Encountered here is part of a vascular system with radially directed primary xylem ribs plus smaller bundles we term “vascular plexus” above. Although primary xylem is comparatively limited, there is much more extensive development of radially aligned tracheids comprising secondary xylem analogous to that observed in lignophytes. What is striking, however, is that this vascular configuration, appearing like what one might normally expect of branch vasculature within the Devonian pseudosporochnaleans (e.g., Stein and Hueber 1989), and indeed how we originally interpreted this tissue, is instead almost entirely comprised of individual rooting appendage traces each following a lax distal course basipetally and outward to the periphery of the trunk. The only possible exceptions to this are the most peripheral strands of the vascular plexus apparently bearing superficial appendage traces in the most acropetal region of the specimen. Unfortunately, however, identity of these outer strands either as rooting appendage traces or cauline bundles cannot be definitely determined. The overall impression one receives is that we probably have not reached entirely cauline portions of the trunk in our permineralization. Evidence from the larger compression of *Eospermatopteris* at South Mountain

(Stein et al. 2007) indicates a change in vascularization between upper regions of the trunk showing discrete longitudinal carbonaceous strands versus a more reticulate pattern observed over portions of the expanded base. Similar patterns are also evident on *Eospermatopteris* casts (see Xu et al. 2017, fig. 1). Therefore, it seems possible, perhaps even likely, that a change in vascularization acropetally perhaps to something developmentally antecedent to that seen in *Xinicaulis* (excluding the latter's root mantle) might be expected in both juvenile and more mature individuals. Unfortunately, this cannot be confirmed with any anatomical evidence from pseudosporochnaleans so far. Thus, how the vascular transition from trunk base bearing the rooting system to aerial branch-bearing trunk is configured and subsequently develops to large size remains an open question.

Possible interpretation of Xenocladia

The fact that the vascular plexus in the acropetal region of our specimen supports interpretation as a closely associated series of rooting appendage traces suggests to us that not all apparent cladoxylopsid anatomy is necessarily cauline (i.e., occurring within the main aerial axis = trunk or its branches). This in turn invites re-appraisal of other material, especially from the New York region, that might be similarly interpreted. In this context, we consider the genus *Xenocladia* as originally described by Arnold (1940, 1952) from Erie County, western New York State. Two specimens are known consisting of pyrite-calcite permineralized tissue fragments. The 1940 specimen came from the Leicester (formerly Tully) Pyrite interpreted to be an anaerobic pyritic lag deposit associated with the unconformity between the Hamilton and Genesee Groups. The latter marks the late Givetian Taghanic marine transgression within the Appalachian basin (Baird and Brett 1986,1991). The more extensively preserved 1952 specimen was collected from the Ludlowville Formation at a horizon not precisely determined but estimated to be 15m (50ft) below the Leicester Pyrite at Caenovia Creek, hamlet of Springbrook, NY. Both occurrences contain plant fragments presumably drifted from emergent land nearby to the north and west, or the Catskill Delta complex further to the east.

In the 1952 specimen (fig. 13*A-B*), outer tissue regions of a sizeable plant are preserved with the stem originally estimated to have been 10cm or more in diameter (Arnold 1952). Elongate xylem bundles lie perpendicular to the curved outer boundary of the specimen and adjacent to many more irregular bundles located toward the inside (fig. 13*B*). All show significant development of secondary xylem (the original defining feature of the genus). The 1940 specimen lacks evidence of an outer boundary and shows fewer bundles, but exhibits more extensive secondary xylem (Arnold 1940).

If tissue fragments of *Xenocladia* represent a vascular plexus of rooting appendage traces similar to that interpreted in our specimen, but from a much larger individual, then it is clear that this system has greatly increased from the presumed juvenile condition as represented by our specimen, with rooting appendage traces much more complexly configured. We suggest that this might be the expected consequence of growth to much larger body size within some pseudosporochnalean, notably coeval *Eospermatopteris* in New York. If comparison is extended to *Eospermatopteris* compressions and casts, then this tissue seems likely to be represented, at least in part, by the carbonaceous strands, probably xylem, in outer portions of the base casts (fig. 13*C-D*). Thus, much of this tissue might also represent portions of a vascular plexus consisting fundamentally of rooting appendage vascularization in both development and function. However even if true, just how this tissue is structured and augmented by new rooting appendages during continued enlargement of the base remains an open question. We note here that larger *Eospermatopteris* casts typically contain thicker strands, suggesting increased secondary xylem over time. The 1940 specimen of *Xenocladia* might represent this condition within a vascular plexus, although a cauline vascular system of the trunk such as seen within the *Xinicaulis* remains a viable alternative. New specimens showing more complete examples of *Xenocladia* tissues would be helpful, especially from the geographic region where originally found. In the meantime, caution is indicated in assigning specimens to *Xenocladia* based upon the presence of secondary xylem alone, but greatly differing otherwise in vascular configuration. It is also important to recognize that there are likely to be important differences

749 within pseudosporochnaleans in vascular anatomy between trunk base bearing rooting appendages, aerial
750 trunk, and modular lateral branches produced from the latter.

751 ***Visualizing juvenile to mature growth in pseudosporochnaleans***

752 The presence of secondary xylem in the vascular plexus and elsewhere in the specimen suggests
753 important involvement of this tissue in the physiology of the juvenile plant, likely increasing in
754 importance during subsequent development to large size. Clearly the need for vascular supply to aerial
755 apex, crown branches, and ever-lengthening trunk must be paramount in a "bipolar" body plan of this
756 type. However, lack of a weight-bearing central column consisting of xylem in the rooting appendage
757 bearing base region, as is commonly encountered in other groups, would seem to represent a structural
758 problem. We suggest that the vascular plexus instead served this function not only in vascular supply to
759 the aerial shoot, but also in accommodating increasing diameter of the trunk and overall structural
760 support.

761 Previous work on *Xinicaulis* (Xu et al. 2017), provided the suggestion that development to large size in
762 this plant involved diffuse meristematic growth in tissues enveloping the vascular system possibly
763 analogous to thickening development in palms although not within discrete meristematic regions. In
764 addition, even though secondary xylem is produced in *Xinicaulis* most notably in the largest vascular
765 bundles of the trunk, secondary xylem by itself seemed insufficient for the structural support for large
766 *Xinicaulis* or *Eospermatopteris* trees without formation of a hollow pith region, the latter to reduce water-
767 filled biomass overall. As a result, a combination of diffuse meristematic growth with progressive
768 hollowing out in the center was previously proposed for both genera along with widening the base
769 possibly due to structural failure under increasing aerial load.

770 Our observations of numerous *Eospermatopteris* specimens certainly support the conclusion that these are
771 internal casts of a hollow trunk and base. A conspicuous reticulate pattern of compressed carbonaceous
772 strands, probably xylem, occurs in continuity on the flat under surface of the cast, around its lateral edges,

773 and continuing upward along the sides of the trunk especially in regions of extended diameter (figs. 11*I*,
774 13*C-D*). In addition, it is interesting to note that nearly every flat undersurface of *Eospermatopteris* casts
775 analyzed to date shows a curious region at its geographic center in which the pattern of carbonaceous
776 strands is either absent or significantly less distinct (fig. 11*I* arrow, *Xu* et al. 2017, their fig. 1*A*).

777 These observations allow for fleshing out a developmental model based on observations detailed here that
778 is tentatively applicable to *Eospermatopteris* and other pseudosprochnaleans (fig. 14). First, it should be
779 noted that the base in our small permineralized specimen with continuous ground tissue, and also in
780 *Lorophyton* compressions, are essentially similar in shape to the much larger casts of *Eospermatopteris*.
781 This suggests close to self-similarity was maintained with increasing size related to diffuse meristematic
782 growth both basipetally and laterally within the base region (fig. 14, gray pattern). We suspect that
783 formation of a hollow center in larger trunks, and possibly also some longitudinal structural failure,
784 played a role in base expansion in response to increasing aerial load over time, as suggested previously.

785 Second, if pseudosporochnalean growth to large size proceeded from the "bipolar" organization seen
786 here, then it seems likely that the pattern of development observed in our specimen was maintained and
787 subsequently elaborated during subsequent growth. However, continued development implies new
788 production of rooting appendages among the older appendages in some way, either with vascularization
789 ending proximally near the hollow trunk center as in our specimen (fig. 14, arrows a), or adventitiously
790 nearer the trunk surface (fig. 14, arrow b), or both. In *Eospermatopteris*, it seems reasonable to imagine
791 continuation of general diffuse meristematic activity in ground/cortical tissues within the laterally
792 extended base and in the aerial trunk, with new rooting appendage vascularization maturing acropetally in
793 appendicular fashion influenced by young appendage apices at or near outer surface. If so, then
794 *Eospermatopteris* casts of the trunk or base center likely preserve part of this pattern but probably not all
795 of it. Observations of *Eospermatopteris* rooting system mounds and *in situ* casts from in the classic
796 Gilboa region (Stein et al. 2021), show many attached rooting appendages diverging directly downward
797 from flattened trunk bases suggesting vigorous appendage development near the base center in large

individuals (fig. 14, arrow c). In addition, many appendages are observed near the extremity of the expanded base (fig. 14, arrow d) suggesting vigorous production in these regions also.

A third point concerns the fact that presumed vascular strands near the periphery in larger *Eospermatopteris* casts must certainly be laterally displaced from positions occupied by similar strands in smaller casts, presumably representing younger individuals. In addition, transverse sections of larger casts indicate not just greater size of individual bundles, likely due to continued secondary xylem development, but also greater total volume and complexity of vascular tissue occupying a greater radial depth (fig. *13C-D,* Boyer 1995) than possible in smaller specimens. Augmentation of these tissues with increased body size is therefore indicated. Moreover, rooting appendages observed on the surface of larger *Eospermatopteris* casts occur far above the level possible in self-similar smaller individuals. Consequently, we suggest that much, if not all, of the anastomosing system of vascular strands observed on the base of large *Eospermatopteris* casts may constitute further development of the vascular plexus, and that most if not all of this is continuous rooting appendage initiation and further development in this *sui generis* organ. Figure 14 represents a greatly simplified view of this process in what is actually observed to be a very complex tissue.

With continued expansion of the trunk base, it is envisioned that more internal parts of the vascular plexus would become less functional and likely displaced or lost due to expansion of the hollow center over time. Since *Eospermatopteris* lacked a solid cylinder of secondary xylem at its base, the structural and functional role of an expanding vascular plexus with new rooting appendage initiation supplemented by continued development of secondary xylem seems critical. This expanding interconnected network of strands, defining and to significant degree constraining the shape of the trunk base would seemingly be required to sustain load and vascular demands of an increasingly distant aerial crown.

Taxonomic disposition

Evidence and rationale that this specimen represents heretofore unknown anatomy and significant stage in the early development of tree architecture within pseudosporochnaleans is presented above. The closest known taxon in terms of size, and overall form is certainly *Lorophyton*, offering a nearly complementary fit. However, the overlap of meaningful diagnostic characters, notably morphology of lateral branches with appendages seen in *Lorophyton* versus internal anatomy observed in the new specimen, is limited. We also recognize that assignment of our specimen to the genus *Lorophyton* has potential paleogeographic implications, especially if generic names are read superficially as location markers. Moreover, distinguishing the juvenile condition of *Pseudosporochnus* in Europe from *Eospermatopteris/Wattieza* in North America based on compression evidence may ultimately prove to be important. As a result, we propose linking this specimen to co-occurring *Eospermatopteris* trees in the Catskill region of New York with possible extension to *Xenocladia* found in marine sediments further west. As in all of paleobotany, the name proposed here hypothesizes an entire plant based on an incomplete set of diagnostic features. Our goal is toward synthesis that resists proliferation of names especially at the generic level. Accordingly, we place our specimen within the genus *Eospermatopteris* as the new species *E. iuvenis*. This approach provides a convenient means to refer to the specimen by name while at the same time reflecting our current thinking about its juvenile condition, most probably of *Eospermatopteris erianus* in North America.

Systematics

Class **Cladoxylopsida** Pichi-Sermolli 1959

Order **Pseudosporochnales** Emberger 1944

Genus ***Eospermatopteris*** Goldring 1924

Eospermatopteris iuvenis *sp. nov.*

Etymology. Latin adjective meaning "youth", used here to describe youthful *Eospermatopteris*.

Diagnosis. Upright plant with main trunk, aerial branches in alternate arrangement, expanded base bearing rooting appendages. Rooting appendages arising at multiple levels on expanded trunk base, appressed to the trunk acropetally, descending directly from the base below. Vascular system of base consisting entirely of rooting appendage traces arising near center of trunk, proceeding laterally and basipetally. Rooting appendage traces with primary xylem commonly enveloped in secondary xylem. Primary xylem compact, comprised of tracheids only. Secondary xylem tracheids in radial files without vascular rays. Ground tissue arenchymatous, with cell walls thinning toward the base.

Type locality. New York State Department of Environmental Conservation quarry, northwest slope of South Mountain, Schoharie County, New York (42° 239' N, 74° 169' W).

Stratigraphy. Oneonta Formation, Genessee Group, Upper Givetian to Lower Frasnian, Devonian.

Holotype. Type specimen main slab assigned NYSM 19,312, with prepared slides here numbered #1-24 assigned NYSM numbers 19,312.1-24 respectively, and slides here numbered #1L-7L assigned NYSM numbers 19,312.35-40 respectively).

Conclusion

At the present time, a coherent interpretation of juvenile form and subsequent development to large size in pseudosporochnaleans may be emerging. The three developmental points mentioned above seem to add significantly to at least *Eospermatopteris*, *Pseudosporochnus* and *Lorophyton*, and might also apply to *Calamophyton* and *Xinicaulis*, but probably not to *Pietzschia*. Whether our visualizations stand up to further evidence remains to be seen. However, it is becoming increasingly clear that it is important to conceive the problem beyond the traditional confines and terminology offered by the telome theory (Zimmermann 1952) or hypothesized developmental processes focused on aerial shoots alone (Stein &

865 Boyer 2006). Instead, what is needed is recognition of the fact that pseudosporochnaleans, and probably
866 most Devonian vascular plants, were far more sophisticated in architecture and integrated in their
867 development than envisioned by traditional telomic processes. In going beyond the telome theory we
868 suggest that an important principle in plant development, yet to be fully exploited in fossil plant
869 reconstructions must be something along the lines of **pay as you grow** (adapted from the very old
870 expression "pay as you go"). By this we mean that in order to survive in the terrestrial environment
871 vascular plants must always have functioned as a coordinated system of apical, lateral, and modular
872 growth intimately tied with equally dynamic development of an acquisition system providing adequate
873 structural support along with water and nutrient supply. In the earliest vascular plants, perhaps
874 represented by those in the Rhynie chert, a continuously developing rhizome bearing determinate and
875 disposable aerial shoots and supplied by continuous acropetal production of rhizoids or adventitious
876 rootlets might have been sufficient to sustain life (Kenrick and Strullu-Derrien 2014, Hetherington and
877 Dolan 2018). However, with increasing size of the plant body in Middle Devonian pseudosporochnaleans
878 it seems almost certain that "pay as you grow" became far more acute. We suggest that despite their
879 remoteness in age and uncertainty about phylogenetic relationships, the opportunity now exists to
880 consider these earliest trees, more fully in this light. Especially important, we believe, is an attempt to
881 integrate both aspects of their "bipolar" body. This in turn leads to analyzing fragmentary evidence, such
882 as seen in *Xenocladia*, with a more unified approach.

883 To date, several developmental models for pseudosporochnaleans have been offered involving different
884 taxa, different forms of preservation, divergent perspectives, and potentially divergent results (Berry and
885 Fairon-Demaret 2002, Meyer-Berthaud et al. 2010, Giesen and Berry 2013, Xu et al. 2017). All models,
886 including a new one advanced here, involve substantial extrapolation from what actually has been
887 observed so far. In our opinion, this is essential in determining where conflicts between views actually lie
888 and providing a testable means to decide between them. New data directly incorporating external
889 morphology with internal anatomy will ultimately be required to develop a more unified and definitive

model. Especially important, we believe, will be direct information relating behavior of meristematic tissues and how development proceeds in the critical transition region between rooting appendage producing trunk base versus branch producing aerial portions of these plants.

Acknowledgments

Work made possible with assistance from John L. Armitage, the New York State Museum, Albany NY, USA, and permission from the New York State Department of Environmental Conservation. CMB's work was supported by Natural Environment Research Council Grant NE/J007897/1. For the purpose of open access, the authors have applied a Creative Commons Attribution (CC BY) license to any Author Accepted Manuscript version arising. We also thank W DiMichele, AMF Tomescu, and anonymous reviewers for very helpful comments.

Literature Cited

Algeo TJ, SE Scheckler 1998 Terrestrial-marine teleconnections in the Devonian: links between the evolution of land plants, weathering processes, and marine anoxic events. Philos Trans R Soc B 353:113-130.

Algeo TJ, SE Scheckler, JB Maynard 2001 Effects of the Middle to Late Devonian spread of vascular land plants on weathering regimes, marine biotas, and global climate. Pages 213-236 *in* PG Gensel, D Edwards, eds, Plants Invade the Land: Evolutionary and Environmental Consequences. Columbia University Press, New York.

Arnold CA 1940 Structure and relationships of some Middle Devonian plants from western New York. Am J Bot 27: 57-63.

Arnold CA 1952 Observations of fossil plants from the Devonian of eastern North America VI *Xenocladia medullosina* Arnold. Contr Mus Paleontol Univ Mich 9:297-309.

Baird GC, CE Brett 1986 Erosion on an anaerobic seafloor: significance of reworked pyrite deposits from the Devonian of New York State. Palaeogeogr Palaeoclimatol Palaeoecol 57:157-193.

Baird GC, CE Brett 1991. Submarine erosion on the anoxic sea floor: statinomic, palaeoenvironmental, and temporal significance of reworked pyrite-bone deposits. Pages 233-257 *in* RV Tyson, TH Pearson, eds, Modern and Ancient Continental Shelf Axoxia. Geol Soc Spec Pub 58.

Banks HP, JD Grierson, PM Bonamo 1985 The flora of the Catskill clastic wedge. Geol Soc Am Spec Paper 201:125-141.

Beck CB 2010. An Introduction to Plant Structure and Development. Cambridge University Press, Cambridge UK.

922 Beck CB, DC Wight 1988 Progymnosperms. Pages 1-84 *in* CB Beck, ed. Origin and Evolution of
923 Gymnosperms. Columbia University Press, New York.

924 Beerling DJ, RA Berner 2005 Feedback and the coevolution of plants and atmospheric CO_2. Proc Natl
925 Acad Sci USA 102:1302-1305.

926 Beerling, DJ 2019 Making Eden. Oxford Univ Press, Oxford UK.

927 Berry CM 2000 A reconsideration of *Wattieza* Stockmans (here attributed to Cladoxylopsida) based on a
928 new species from the Devonian of Venezuela. Rev Palaeobot Palynol 112:125-146.

929 Berry CM 2019 Paleobotany: the rise of the Earth's early forests. Current Biology 29:R790-R807.

930 Berry CM, M Fairon-Demaret 1997 A reinvestigation of the cladoxylopsid *Pseudosporochnus nodosus*
931 Leclercq et Banks from the Middle Devonian of Goé, Belgium. Int J Plant Sci 158:350-372.

932 Berry CM, M Fairon-Demaret 2002 The architecture of *Pseudosporochnus nodosus* Leclercq et Banks: a
933 Middle Devonian Cladoxylopsid from Belgium. Int J Plant Sci 163:699-713.

934 Berry CM, WE Stein 2000 A new Iridopteridalean from the Devonian of Venezuela. Int J Plant Sci
935 161:807-827.

936 Berry CM, WE Stein, J Cordi 2022 A new reconstruction of the iridopteridalean *Ibyka amphikoma* Skog
937 et Banks from the Middle Devonian of Gilboa, New York State. Int J Plant Sci 183:450-464.

938 Berry CM, Y Wang 2006 A new plant attributed to Cladoxylopsida from the Middle Devonian of Yunnan
939 Province, China. Rev Palaeobot Palynol 142:63-78.

940 Boyce CK, WA DiMichele 2016 Arborescent lycopsid productivity and lifespan: constraining the
941 possibilities. Rev Palaeobot Palynol 227:97-110.

942 Boyer JS 1995 Reexamination of *Eospermatopteris eriana* (Dawson) Goldring from the upper Middle
943 Devonian (=Givetian) Flora at Gilboa, New York. MS diss. Southern Illinois University,
944 Carbondale, IL.

945 Carluccio LM, FM Hueber, HP Banks 1966 *Archaeopteris macilenta*, anatomy and morphology of its
946 frond. Am J Bot 53:719-730.

947 Davies NS, MR Gibling, MC Rygel 2011 Alluvial facies evolution during the Palaeozoic greening of the
948 continents: case studies, conceptual models and modern analogues. Sedimentology 58:220-258.

949 Dawson JW 1871 On new tree ferns and other fossils from the Devonian. Quart J Geol Soc London
950 27:269-275.

951 DeMason DA 1983 The primary thickening meristem: definition and function in monocotyledons. Am J
952 Bot 70:955-962.

953 DiMichele WA, RM Bateman, GW Rothwell, IAP Duijnstee, SD Elrick, CV Looy 2022 *Stigmaria*: a
954 review of the anatomy, development, and functional morphology of the rootstock of the
955 arboreous lycopsids. Int J Plant Sci 183:493-534.

956 Doyle JA, M.J. Donoghue 1986 Seed plant phylogeny and the origin of angiosperms: an experimental
957 cladistic approach. Bot Rev 52:331-429.

958 Durieux T, MA Lopez, AW Bronson, AMF Tomescu 2021 A new phylogeny of the cladoxylopsid
959 plexus: contribution of an early cladoxylopsid from the Lower Devonian (Emsian) of Quebec.
960 Am J Bot 108:2066-2095.

961 Emberger L 1944 Les plantes fossils dans leurs rapports avec les végétaux vivant. Masson Paris.

962 Fairon-Demaret M, CS Li 1993 *Lorophyton goense* gen. et sp. nov. from the Lower Givetian of Belgium
963 and a discussion of the Middle Devonian Cladoxylopsida. Rev Palaeobot Palynol 77:1-22.

964 Galtier J, FM Hueber 2001 How early ferns became trees. Proc R Soc London B 268:1955-1957.

965 Giesen P, Berry CM 2013 Reconstruction and growth of the early tree *Calamophyton*
966 (Pseudosporochnales, Cladoxylopsida) based on exceptionally complete specimens from Lindlar,
967 Germany (Mid-Devonian): Organic connection of *Calamophyton* branches and *Duisbergia*
968 trunks. Int J Plant Sci 174: 665-686.

969 Goldring W 1924 The Upper Devonian forest of seed ferns in eastern New York. New York State
970 Museum Bulletin, Report of the Director 251:50–92.

971 Goldring W 1927 The oldest known petrified forest. Sci Monthly 24:514-529.

972 Groff PA, DR Kaplan 1988 The relation of root systems to shoot systems in vascular plants. Bot Rev
973 54:387-422.

974 Hetherington AJ, L Dolan 2018 Stepwise and independent origins of roots among land plants. Nature
975 561:235-238.

976 Hetherington AJ, CM Berry, L Dolan 2020 Multiple origins of dichotomous and lateral branching during
977 root evolution. Nature Plants 6:454-459.

978 Hueber FM 1961 *Hepaticites devonicus* a new fossil liverwort from the Devonian of New York. Ann Mo
979 Bot Gdn 48:125-131.

980 Hueber FM, HP Banks 1979 *Serrulacaulis furcatus* gen. et sp. nov., a new zosterophyll from the lower
981 upper Devonian of New York State. Rev Palaeobot Palynol 28:169-189.

982 Kenrick P, C Strullu-Derrien 2014 The origin and early evolution of roots. Plant Phys 166:570-580.

983 Leclercq S, HP Banks 1962 *Pseudosporochnus nodosus* sp. nov., a Middle Devonian plant with
984 Cladoxylalean affinities. Palaeontogr Abt B 110:1-34.

985 Leclercq S, KM Lele 1968 Further investigation on the vascular system of *Pseudosporochnus nodosus*
986 Leclercq et Banks. Palaeontogr Abt B 123:97-112.

987 Lemoigne Y, A Iurina 1983 *Xenocladia medullosina* Ch. A. Arnold (1940) 1952 du Dévonien moyen du
988 Kazakhstan (URSS). Geobios 16:513-547.

989 Meyer-Berthaud B, A Soria, GC Young 2007 Reconsidering differences between Cladoxylopsida and
990 Iridopteridales: evidence from *Polyxylon australe* (Upper Devonian, New South Wales,
991 Australia). Int J Plant Sci 168:1085-1097.

992 Meyer-Berthaud B, SE Scheckler, J Wendt 1999 *Archaeopteris* is the earliest known modern tree. Nature
993 398:700-701.

994 Meyer-Berthaud B, A Soria, GC Young 2007 Reconsidering differences between Cladoxylopsida and
995 Iridopteridales: evidence from *Polyxylon australe* (Upper Devonian, New South Wales,
996 Australia). Int J Plant Sci 168:1085-1097.

997 Meyer-Berthaud B, A Soria, AL Decombeix 2010 The land plant cover in the Devonian: A reassessment
998 of the evolution of the tree habit. Pages 59-70 *in* M Vecoli, G Clément, B Meyer-Berthaud, eds. The
999 Terrestrialization Process: Modelling Complex Interactions at the Biosphere-Geosphere Interface. Vol
1000 339, Geol Soc London.

1001 Mustafa H 1978 Beiträge zur Devonflora. III. Argumenta Palaeobot 5:91-132.

1002 Pan Y, RA Birdsey, OL Phillips, RB Jackson 2013 The structure, distribution, and biomass of the world's
1003 forests. Ann Rev Ecol Evol Syst 44:593–62.

1004 Pichi-Sermolli R 1959 Pteridophyta. Pages 421-493 *in* WB Turrill ed. Vistas in Botany. Pergamon,
1005 London.

1006 Pigg KB 1992 Evolution of Isoetalean lycopsids. Ann Mo Bot Gdn 79:589-612.

1007 Pigg KB 2001 Isoetalean lycopsid evolution: from the Devonian to the present. Am Fern J 91:99-114.

1008 Pigg KB, GW Rothwell 1979 Stem-root transition of an Upper Pennsylvanian woody lycopsid. Am J Bot
1009 66:914-924.

1010 Platt JR 1964 Strong inference. Science 146:347-353.

1011 Rothwell GW, SE Wyatt, AMF Tomescu 2014 Plant evolution at the interface of paleontology and
1012 developmental biology: an organism-centered paradigm. Am J Bot 101: 899-913.

1013 Rudall P 1991 Lateral meristems and stem thickening growth in monocotyledons. Bot Rev 57:150-163.

1014 Sanders H, GW Rothwell, SE Wyatt 2011 Parallel evolution of auxin regulation in rooting systems. Plant
1015 Syst Evol 291:221-225.

1016 Scotland RW 2010 Deep homology: a view from systematics. Bioessays 32:438-449.

1017 Sevon WD, DL Woodrow 1985 Middle and Upper Devonian stratigraphy within the Appalachian basin.
1018 Pages 1-7 *in* DL Woodrow, WD Sevon, eds, The Catskill Delta. Geol Soc Am Spec Pap 201,
1019 Boulder CO, USA.

1020 Shubin N, C Tabin, S Carroll 1997 Fossils, genes and the evolution of animal limbs. Nature 388:639-648.

1021 Soria A, B Meyer-Berthaud 2003 Occurrence of whorled organotaxis in the cladoxylopsid *Pietzschia*
1022 *polyupsilon* Read and Campbell (Lower Carboniferous, USA). Rev Palaeobot Palynol 124:29-49.

1023 Soria A, B Meyer-Berthaud 2004 Tree fern growth strategy in the late Devonian cladoxylopsid species
1024 *Pietzschia levis* from the study of its stem and root system. Am J Bot 91:10-23.

1025 Soria A, B Meyer-Berthaud 2005 Reconstructing the late Devonian cladoxylopsid *Pietzschia schulleri*
1026 from new specimens from southeastern Morocco. Int J Plant Sci 166:857-874.

1027 Soria A, B Meyer-Berthaud, SE Scheckler 2001 Reconstructing the architecture and growth habit of
1028 *Pietzschia levis* sp. nov. (Cladoxylopsida) from the Late Devonian of southeastern Morocco. Int J
1029 Plant Sci 162:911-926.

1030 Stein WE 1987 Phylogenetic analysis and fossil plants. Rev Palaeobot Palynol 50:31-61.

1031 Stein WE, FM Hueber 1989 The anatomy of *Pseudosporochnus*: *P. hueberi* from the Devonian of New
1032 York. Rev Palaeobot Palynol 60:311-359.

1033 Stein WE, CM Berry, LV Hernick, F Mannolini 2012 Surprisingly complex community discovered in the
1034 mid-Devonian fossil forest at Gilboa. Nature 483:78-81.

1035 Stein WE, CM Berry, LV Hernick, F Mannolini F 2021 The classic mid-Devonian *Eospermatopteris*
1036 localities, Gilboa NY, USA. Rev Palaeobot Palynol 295:104520.

1037 Stein WE, CM Berry, LV Hernick, F Mannolini F 2022 Root-bearing portions of a young
1038 pseudosporochnalean from the Catskill delta complex of New York. Mendeley Data V1:
1039 DOI: 10.17632/st29d98fhp.1

1040 Stein WE, CM Berry, JL Morris, LV Hernick, F Mannolini, C Ver Straeten, E Landing, CH Wellman, DJ
1041 Beerling, JR Leake 2020 Mid-Devonian *Archaeopteris* Roots Signal Revolutionary Change in
1042 Earliest Fossil Forests. Current Biology 30:421-431.

1043 Stein WE, JS Boyer 2006 Evolution of land plant architecture: beyond the telome theory. Paleobiology
1044 32:450-482.

1045 Stein WE, F Mannolini, LV Hernick, E Landing, CM Berry 2007 Giant cladoxylopsid trees resolve the
1046 enigma of the Earth's earliest forest stumps at Gilboa. Nature 446:904-907.

1047 Stein WE, DC Wight, CB Beck 1982 Techniques for preparation of pyrite and limonite
1048 permineralizations. Rev Palaeobot Palynol 36:185-194.

1049 Stevenson DW 1980 Radial growth in the Cycadales. 1980 Am J Bot 67:465-475.

1050 Toledo S, AC Bippus, AMF Tomescu 2018. Buried deep behind the veil of extinction: euphyllophyte
1051 relationships at the base of the spermatophyte clade. Am J Bot 105:1264-1285.

1052 Traverse A, A Schuyler 1994 Palynostratigraphy of the Catskill and part of the Chemung magnafacies,
1053 southern New York State, USA. Courier Forschungsinstitut Senckenberg 169:261–274.

1054 Ver Straeten C 2009 The classic Devonian of the Catskill Front: a foreland basin record of Acadian
1055 orogenesis. NYSGA Field Trip Guidebook 81st Meeting: 7.1-7.54.

1056 Xu H-H, CM Berry, WE Stein, Y Wang, P Tang, Q Fu 2017 Unique growth strategy in the Earth's first
1057 trees revealed in silicified fossil trunks from China. Proc Nat Acad Sci USA 114:12009-12014.

1058 Xue J, S Hao, JF Basinger 2010 Anatomy of the late Devonian *Denglongia hubeiensis*, with a discussion
1059 of the phylogeny of the Cladoxylopsida. Int J Plant Sci 171:107-120.

1060 Zimmermann W 1952 Main results of the "telome theory". The Paleobotanist, Birbal Sahni Memorial
1061 Volume: 456-470.

1062

Figure Descriptions

Fig. 1 Impression evidence of small pseudosporochnalean trunk with attached rooting appendages: NYSM 19,312. *A*, Overall view; right-facing arrows indicate branch insertions; left-facing arrow possible branch insertion, see fig. 2 for interpretation, scale bar = 30mm. *B*, Possible branch system with central axis and indistinct attached lateral appendages found on same surface as *A*, but not attached, scale bar = 10mm. *C*, Pyrite nodule with anatomical detail in place as observed in the field; ridges on nodule and impression are an exact fit, scale bar = 30mm.

Fig. 2 *A*, Diagrammatic representation of trunk impression with expanded base and attached rooting appendages shown in fig. 1*A*. Part of trunk base in contact with pyrite nodule, a, aerial shoot, b. Insertion of lateral branches, black triangles, uncertain branch insertion, lighter triangle, scale bar = 30mm. *B*, Plan of sections cut from the pyrite nodule. Transverse wafers 1-18 procede from the apical end. Transverse wafers 19R-24R continue the series for half of base, R. Longitudinal wafers 1L-8L procede from center to outside edge of other half of base, L. Individual transverse wafer surfaces, b, f, as in Fig. 3 and 4.

Fig. 3 Interpretation of the vascular system, numbers refer to transverse wafers cut at 2mm intervals with f=front and b=back surfaces as mounted on the slides. Colored circles indicate vascular bundles traced through the series of sections often with distal dichotomies. Top of each section drawing represents the back surface of the pyrite nodule as displayed in Figs. 1C & 2B, with all b drawings flipped horizontally for consistent perspective, scale bar at 18f = 4mm.

Fig. 4 Interpretation of the vascular system near the base of the specimen, section numbers 19R-24R continue the transverse series in fig. 2*B* toward specimen base for half of the specimen, colored circles indicate different vascular bundles traced through the series. Section numbers 1L-7L are longitudinal section surfaces from center line normal to bedding plane outward, f=front and b=back surfaces, with b drawings flipped horizontally for consistent perspective, scale bar = 4mm.

Fig. 5 Pyrite nodule showing general anatomical features; all scale bars = 2mm. *A-E*, Representative transverse sections showing changes in vascular system and increase in size proceeding toward the trunk base; compare figs. 2-3. *A*, 5f. *B*, 9b image reversed, arrow a = outer ground tissue region, arrow b = inner ground tissue region. *C*, 18f. *D*, 21Rf, arrows indicate arcuate bands representing rooting appendages at the surface of the permineralization. *E*, 24Rb image reversed, arrow indicates amorphous pyrite region with xylem in the center representing rooting appendage trace or entire rooting appendage. *F-G*, Pyrite nodule before wafers were cut; maximum diameter of nodule = 32mm, compare fig. 1*C*. *H-K*, Representative longitudinal sections at basal end of the permineralization proceeding from midline to outer extremity; compare fig. 3. *H*, 1Lb image reversed. *I*, 3Lf. *J*, 4Lb image reversed, arrows indicate rooting appendage. *K*, 6Lf, arrow indicates rooting appendage(s).

Fig. 6 Vascular system in apical region of the specimen; arrows a-k indicate the same rooting appendage trace in each photograph. *A-C*, Transverse views showing configuration of the vascular plexus consisting of multiple vascular bundles each containing multiple rooting appendage traces, scale bars = 1mm. *A*, 3f. *B*, 5b image reversed, arrows indicate expanded tips of radially oriented vascular strands with abundant secondary xylem preserved in limonite. *C*, 5f rooting appendage derived from division of a radial strand. *D-F*, Serial transverse views of rooting appendage indicated in *C*, scale bars = 0.5mm. *D*, Level showing departure of trace, arrow. *E*, Separated trace with vascular tissues inside amorphous pyrite, arrow. *F*, 6f distal view with arrow indicating arcuate band of compressed organic matter representing the rooting appendage compression at this level.

Fig. 7 Vascular system showing diminution of vascular bundles within the vascular plexus in the basipetal direction and the course of rooting appendage traces at this level in the trunk; arrows a-k continue trace identification in fig. 6. *A-D*, Progressively basipetal views in transverse section, arrows c-k indicate specific rooting appendage traces described in the text, scale bars = 2mm. *A*, 7f. *B*, 8f. *C*, 9f. *D*, 10f. *E-H*, Serial views of trace system indicated by arrows k, showing distal course of rooting appendage traces in the basipetal direction, scale bars = 0.5mm. *E*, 3f rooting appendage trace at level in *A* proximal

to dichotomy. *F*, 5f rooting appendage trace at level of dichotomy. *G*, 8f two rooting appendage traces at level in *B*. *H*, rooting appendage traces near periphery at level in *D*.

Fig. 8 Vascular system in mid to basal portions of the trunk; arrows a-k continue trace identification in figs. 6-7 whereas arrows l-o indicate traces observed in this region. *A-D*, Serial wafer views, arrows e, g, and i-o indicate individual rooting appendage traces often with dichotomies at different levels as described in the text, scale bars = 2mm. *A*, 11f. *B*, 13f. *C*, 14f. *D*, 17b image reversed. *E-G*, Serial views at higher magnification of trace system indicated by arrows l, scale bars = 0.5mm. *E*, 11f Multiple traces at level in *A* enclosed within secondary xylem. *F*, 13f level in *B*. *G*, 14f Right hand derivative rooting appendage trace of the trace group l in *C*.

Fig. 9 Rooting appendage trace details mid to basal portions of the trunk; arrows n-o continue trace identification in fig. 8, scale bars = 0.5mm. *A-D*, Serial views in higher magnification of trace system indicated by arrows n in fig. 8. *A*, 11f. *B*, 13f. *C*, 14f. *D*, 17b image reversed. *E-I*, Serial views in higher magnification of trace system indicated by arrows o in fig. 8. *E*, 14b image reversed. *F*, 15f. *G*, 16b image reversed. *H* 17b image reversed. *I*, 18f.

Fig. 10 Histological features of primary and secondary xylem. *A*, 5f Radially elongate vascular bundle in apical region of the specimen showing extensive secondary xylem and apparently elongate primary xylem, scale bar = 0.2mm. *B*, 10f Elliptical vascular bundle near periphery of specimen in transverse section comprised of two rooting appendage traces arrows, scale bar = 0.2mm. *C*, 1Lf Rooting appendage trace with more extensive surrounding amorphous pyrite in longitudinal section, scale bar = 0.2mm. *D*, 24Rb Rooting appendage trace with surrounding amorphous pyrite in transverse section, scale bar = 0.5mm. *E*, 2Lb Detail of rooting appendage trace in longitudinal section showing arrangement of tracheids and pitting in both primary and secondary xylem, scale bar = 0.2mm.

Fig. 11 Histological details of xylem and ground tissues. *A-E*, Serial transverse views tracing a small centrally located rooting appendage trace, arrows, in the acropetal direction, scale bars = 0.5mm. *A*, 10b

image reversed; *B*, 9f; *C*, 9b image reversed; *D*, 8f; *E*, 8b image reversed. *F-G*, Serial transverse views of outer ground tissue showing differences in cell shapes and wall thicknesses, scale bars = 0.2mm. *F*, 5f; *G*, 18f; *H*, 4Lf longitudinal view of peripheral ground tissue, scale bar = 0.2mm. *I*, *Eospermatopteris* cast in NYSM showing flat basal surface with central region showing lesser preservation, arrow.

Fig. 12 Interpretation of general features of rooting appendage vascularization in the observed specimen in longitudinal section. Diffuse meristematic activity primarily in the expanded rooting appendage region of the trunk, grey pattern. Rooting appendage traces, black, with rooting appendage divergence in the basipetal direction and development of secondary xylem indicated by thickness of trace lines. Close association of rooting appendage traces with secondary xylem constitute the vascular plexus observed both acropetally and near the base.

Fig. 13 *A-B*, *Xenocladia medullosina* Arnold (Arnold 1952) portion of the specimen in Binghamton University Collection (NYSM) embedded in plastic, originally donated by Arnold. *A*, Transverse section, scale bar = 5 mm. *B*, magnification of *A* showing outer ring of radially elongate xylem and more internal bundles both with secondary xylem, scale bar = 2 mm. *C-D*, *Eospermatopteris* casts in sectional views, NYSM collection. *C*, Longitudinal section showing embedded presumed vascular strands flaring outward toward the base, NYSM E373f, scale bar = 20 mm. *D*, Transverse section showing complex system of presumed vascular strands along preserved periphery top and left, NYSM E203, scale bar = 20 mm.

Fig. 14 Hypothetical development of vascular plexus in larger *Eospermatopteris* individuals with hollow center in longitudinal section. Diffuse meristematic activity greatest in the expanded rooting appendage region of the trunk, grey pattern, and diminishing acropetally. Rooting appendage traces, black, with secondary xylem development within the vascular plexus indicated by thickening. Although shown as a single layer here, the vascular plexus seems likely to become greater in radial dimension and augmented in complexity via extended development. Rooting appendage traces end blindly toward the interior, a, but

also arise externally, b. Regions in *Eospermatopteris* casts and paleosol footprints that show numerous rooting appendages are at base center, c, and near the base extremity, d.

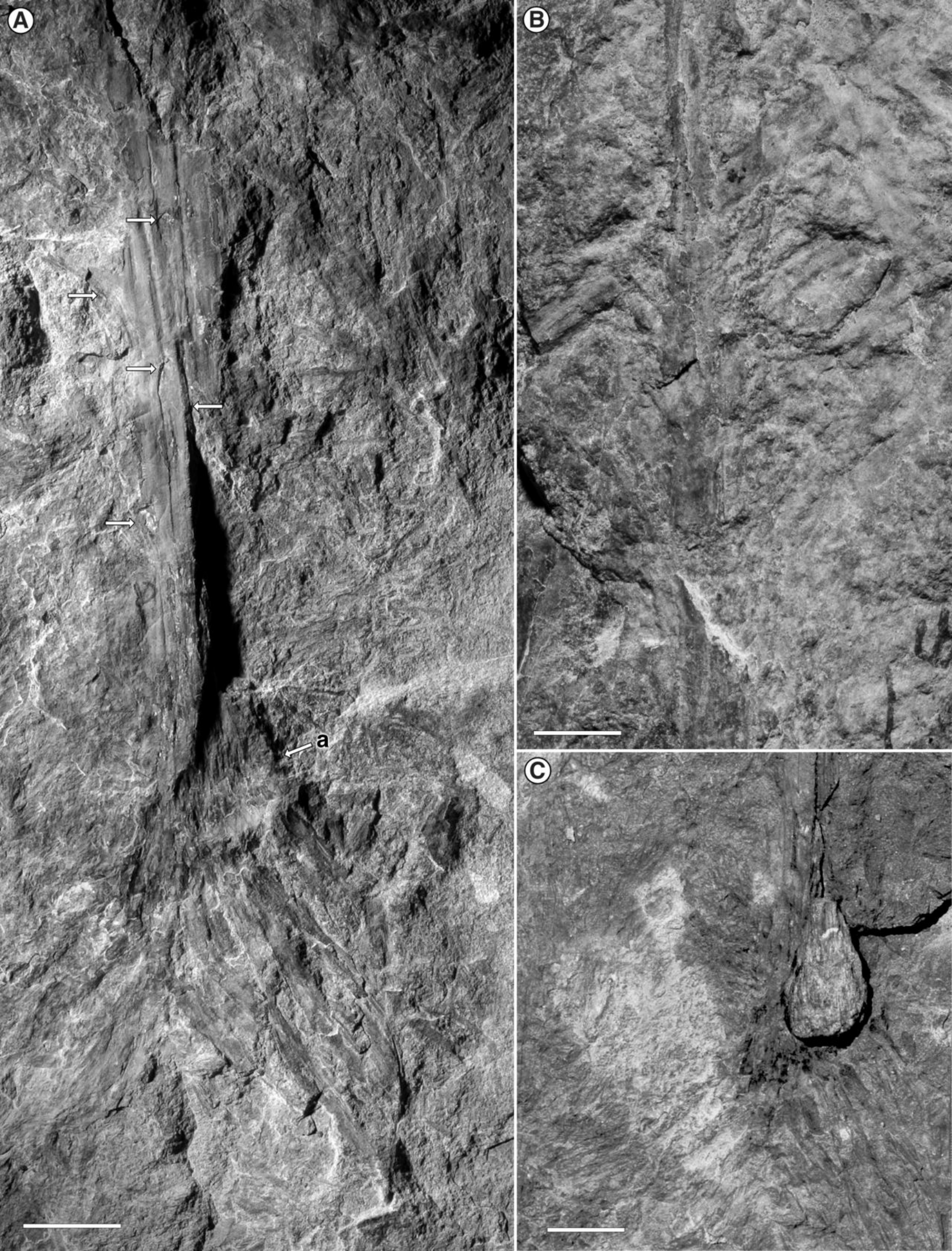
A
B
C
a

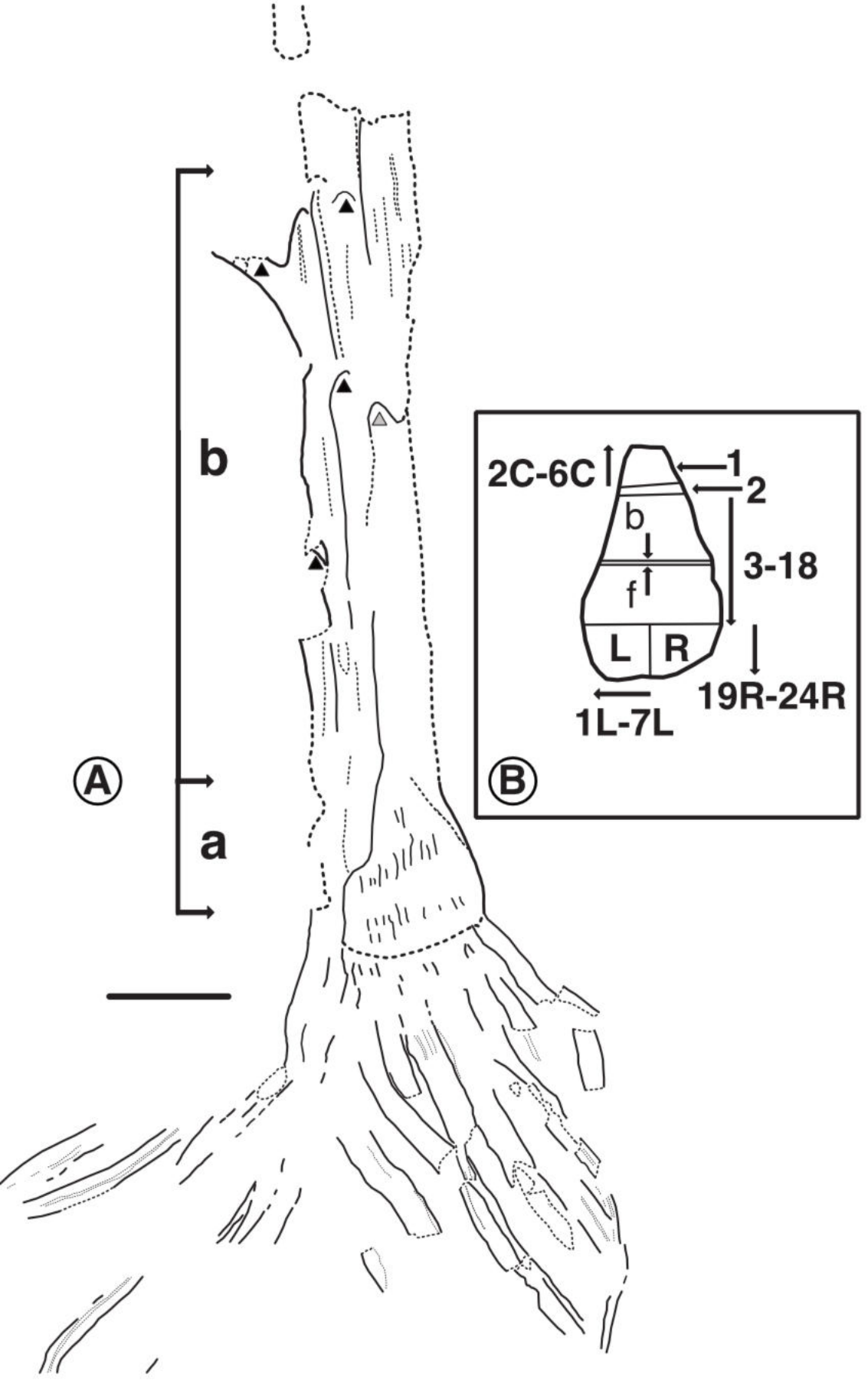
b
a
A
2C-6C
1
2
b
f
3-18
L
R
19R-24R
1L-7L
B

3b
7b
11b
15b
3f
7f
11f
15f
4b
8b
12b
16b
4f
8f
12f
16f
5b
9b
13b
17b
5f
9f
13f
17f
6b
10b
14b
18b
6f
10f
14f
18f

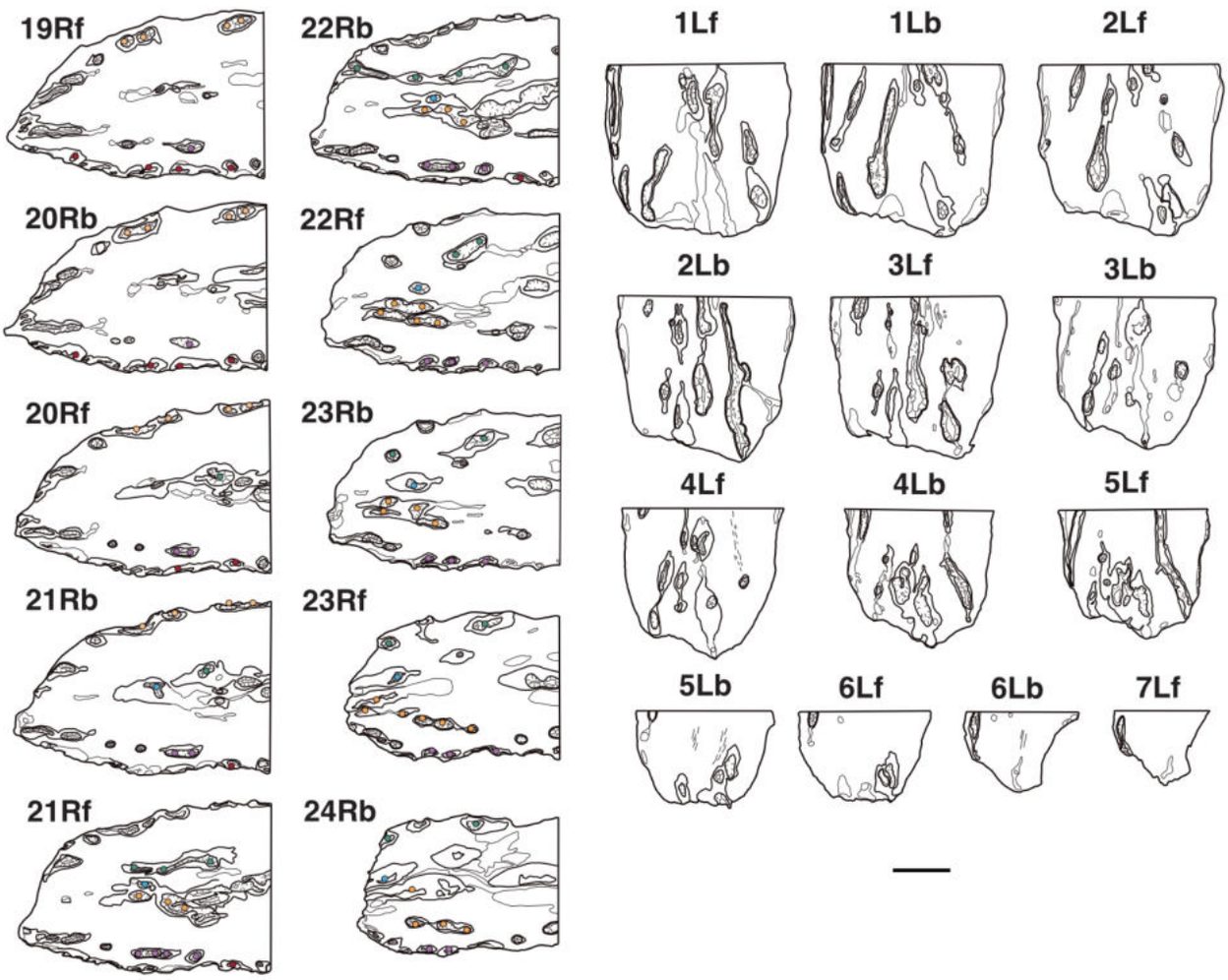
19Rf
22Rb
20Rb
22Rf
20Rf
23Rb
21Rb
23Rf
21Rf
24Rb
1Lf
1Lb
2Lf
2Lb
3Lf
3Lb
4Lf
4Lb
5Lf
5Lb
6Lf
6Lb
7Lf

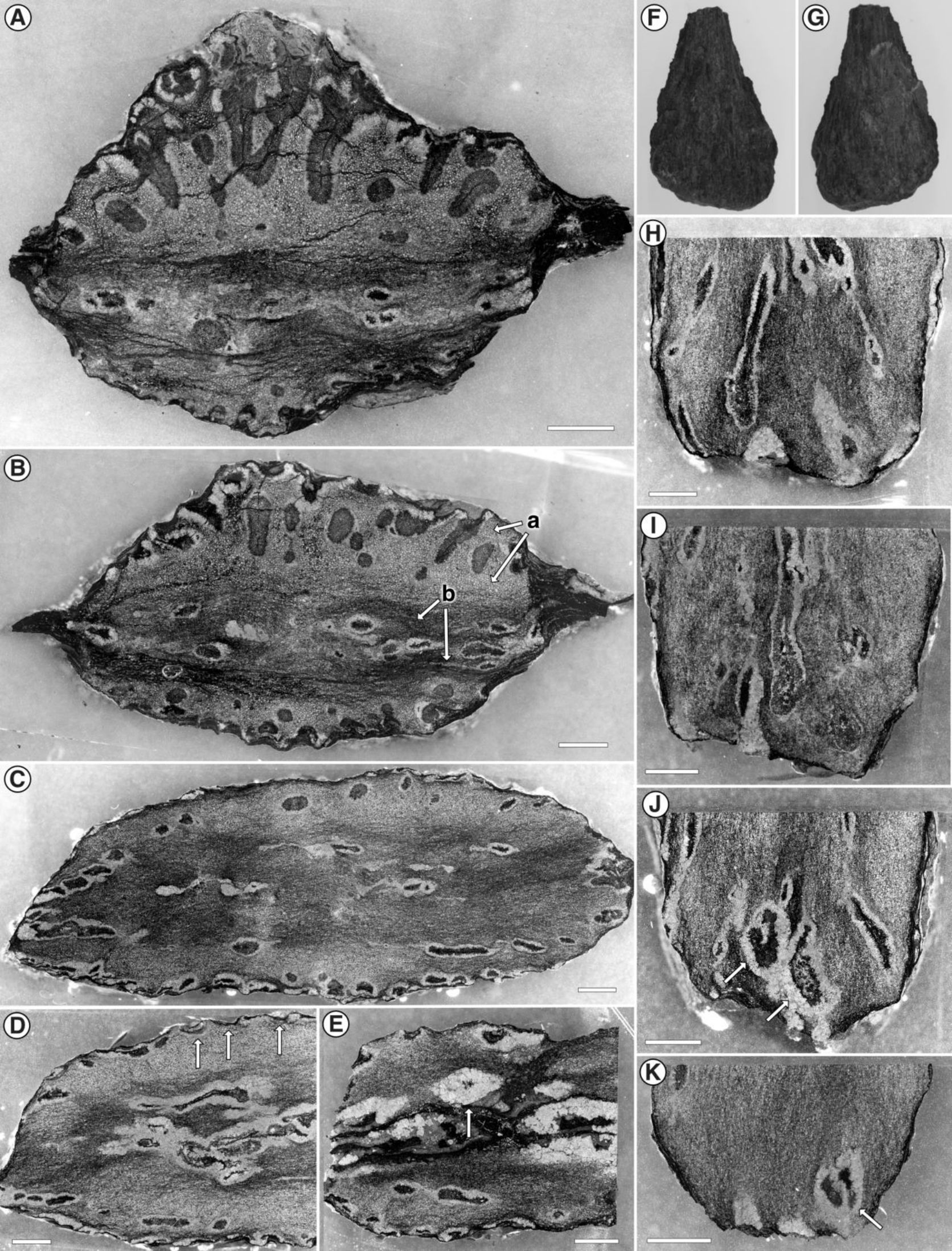
A
B
a
b
C
D
E
F
G
H
I
J
K

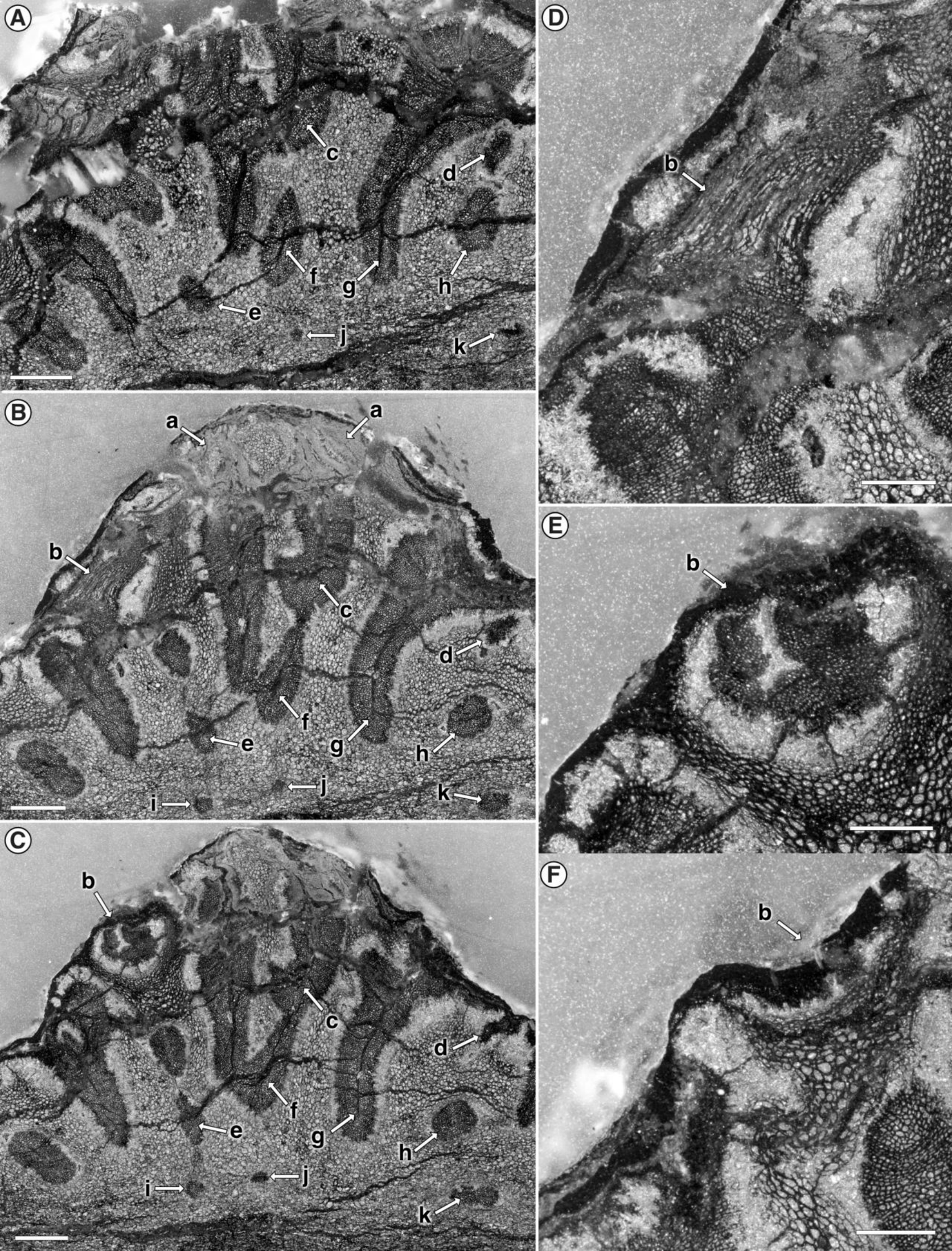
A
c
d
f
g
h
e
j
k
B
a
a
b
c
d
f
g
h
e
j
i
k
C
b
c
d
f
g
h
e
j
i
k
D
b
E
b
F
b

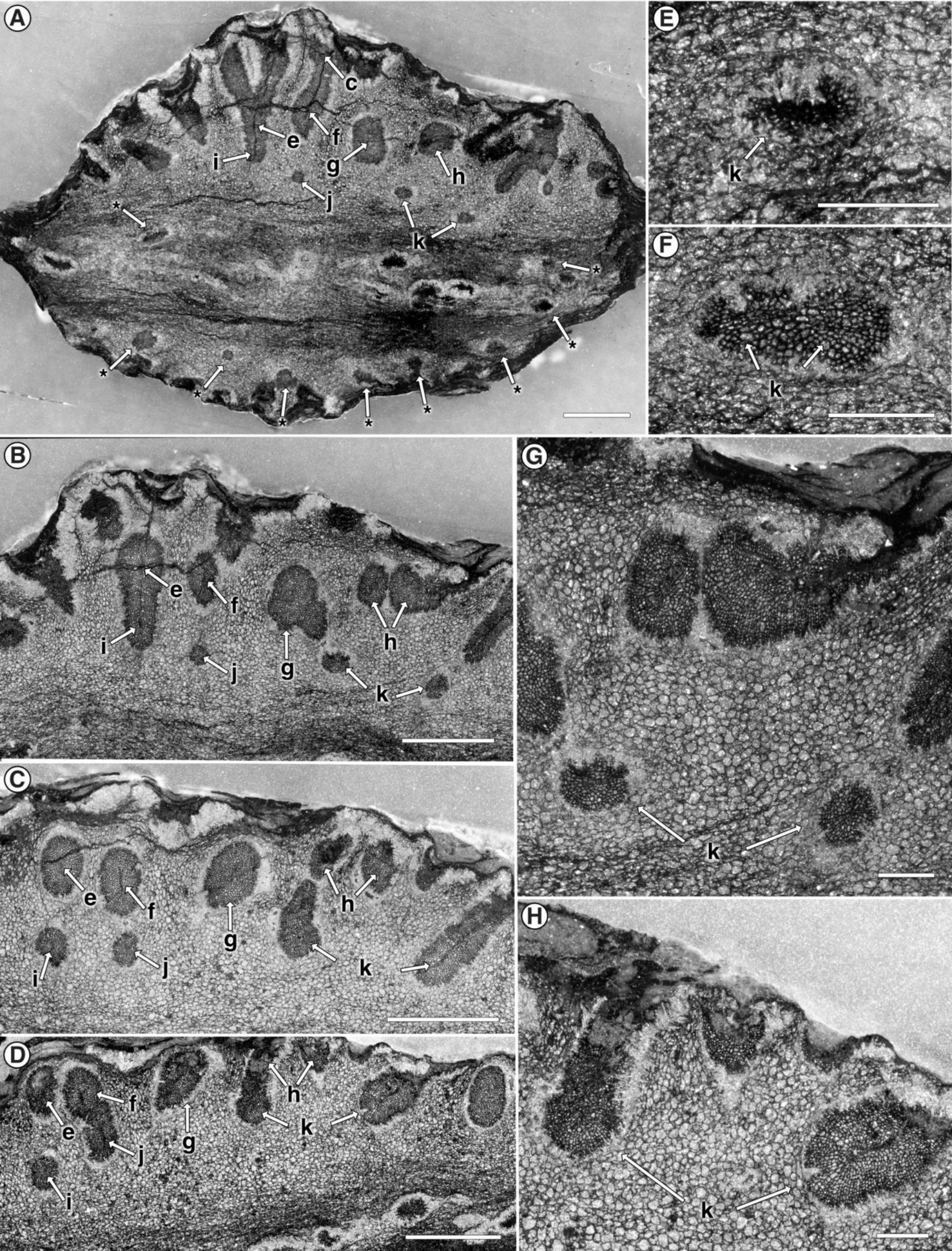
A
c
e
f
i
g
h
j
k
*
B
e
f
i
h
j
g
k
C
e
f
g
h
i
j
k
D
f
h
e
g
k
j
i
E
k
F
k
G
k
H
k

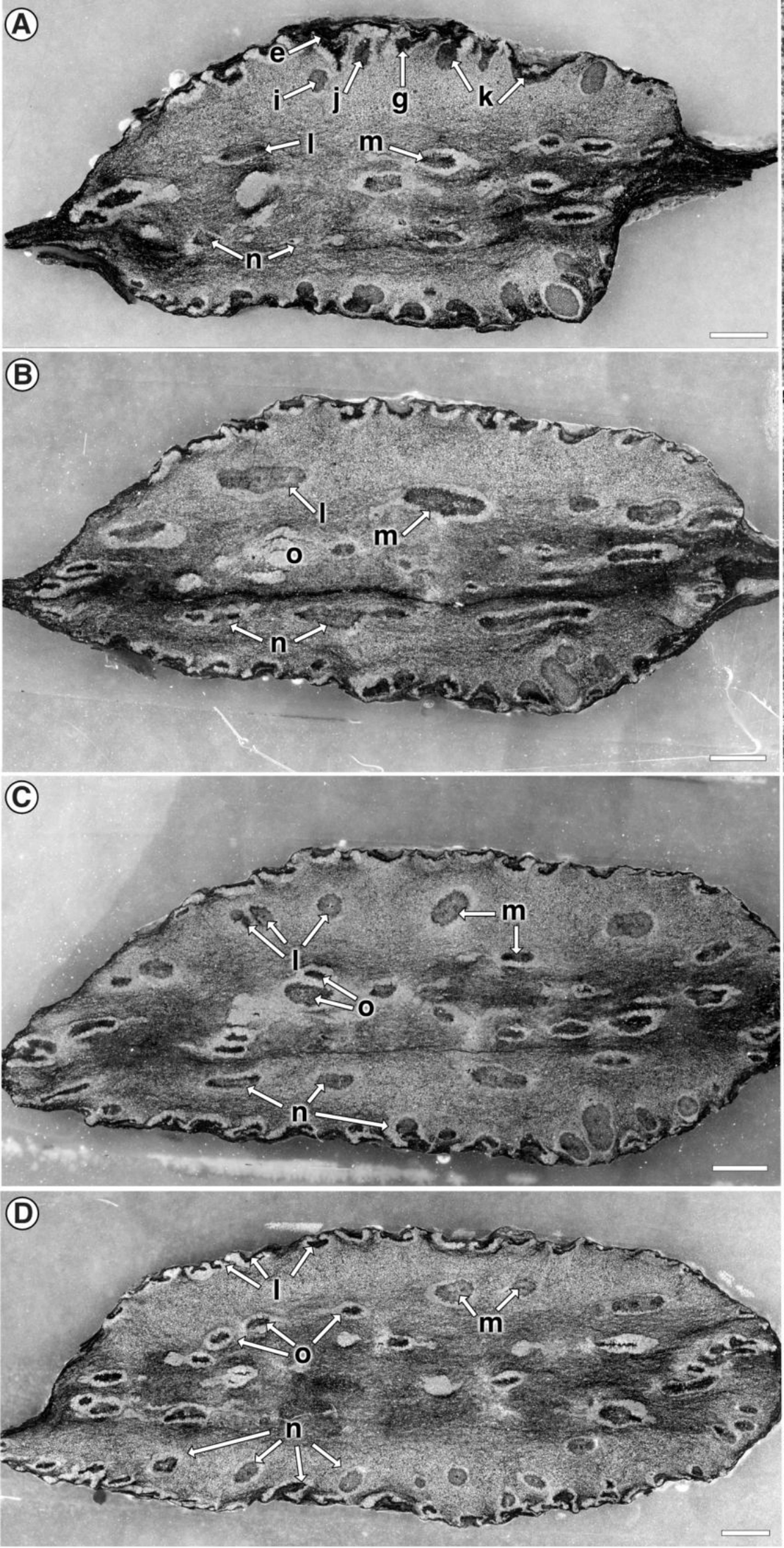
A
e
i
j
g
k
l
m
n
B
l
m
o
n
C
m
l
o
n
D
l
m
o
n

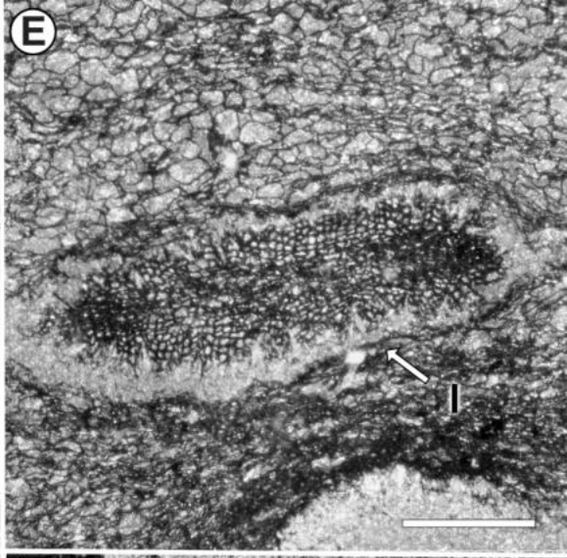
E
l

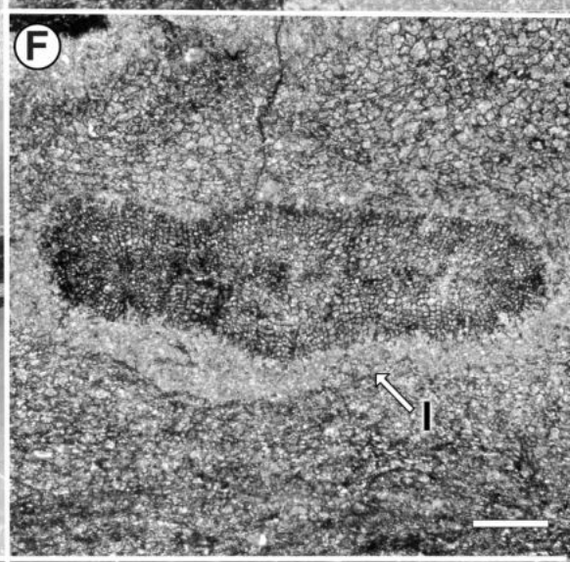
F
l

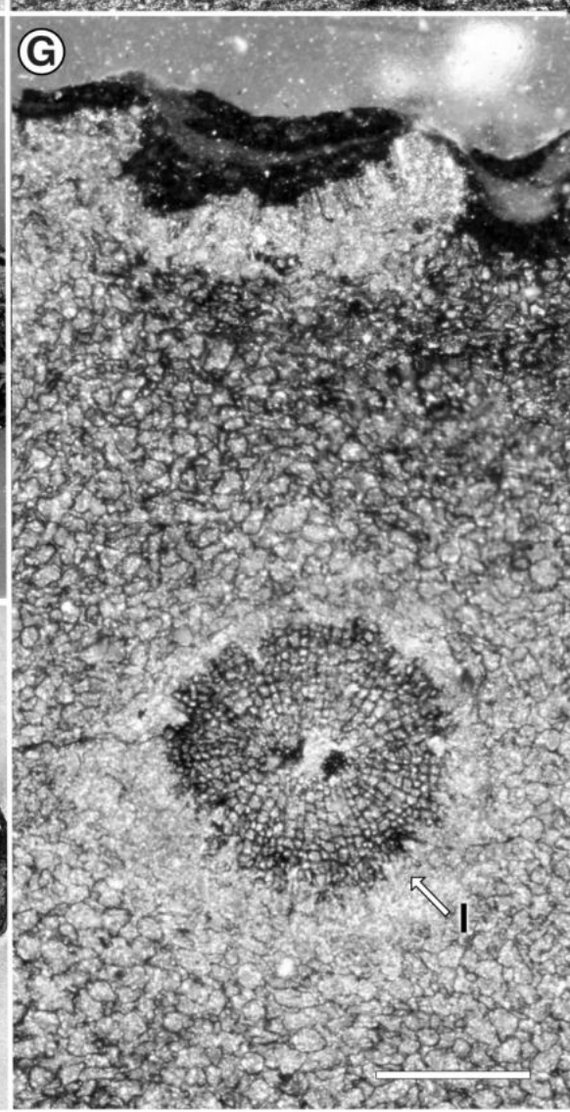
G
l

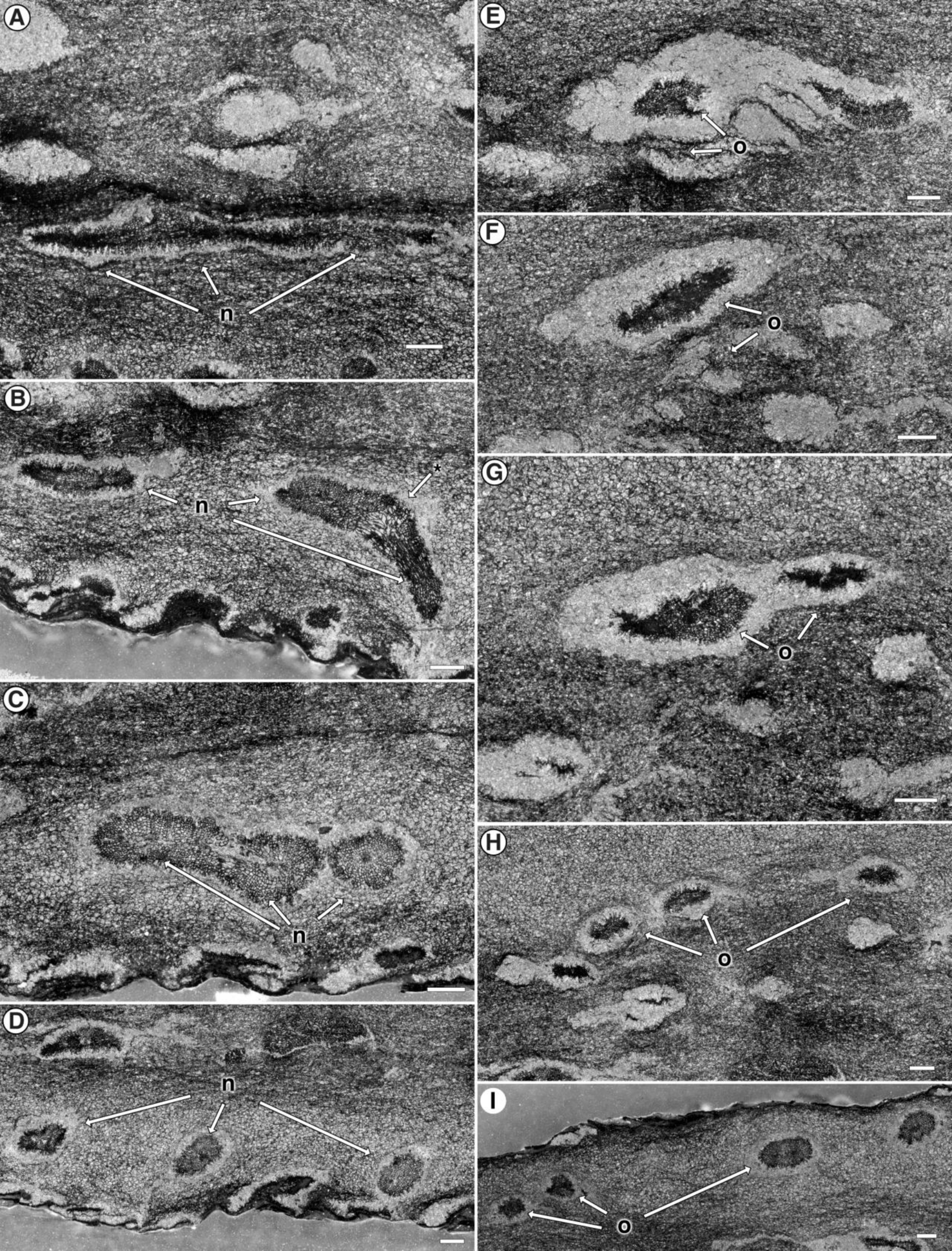
A
n
B
n
*
C
n
D
n
E
o
F
o
G
o
H
o
I
o

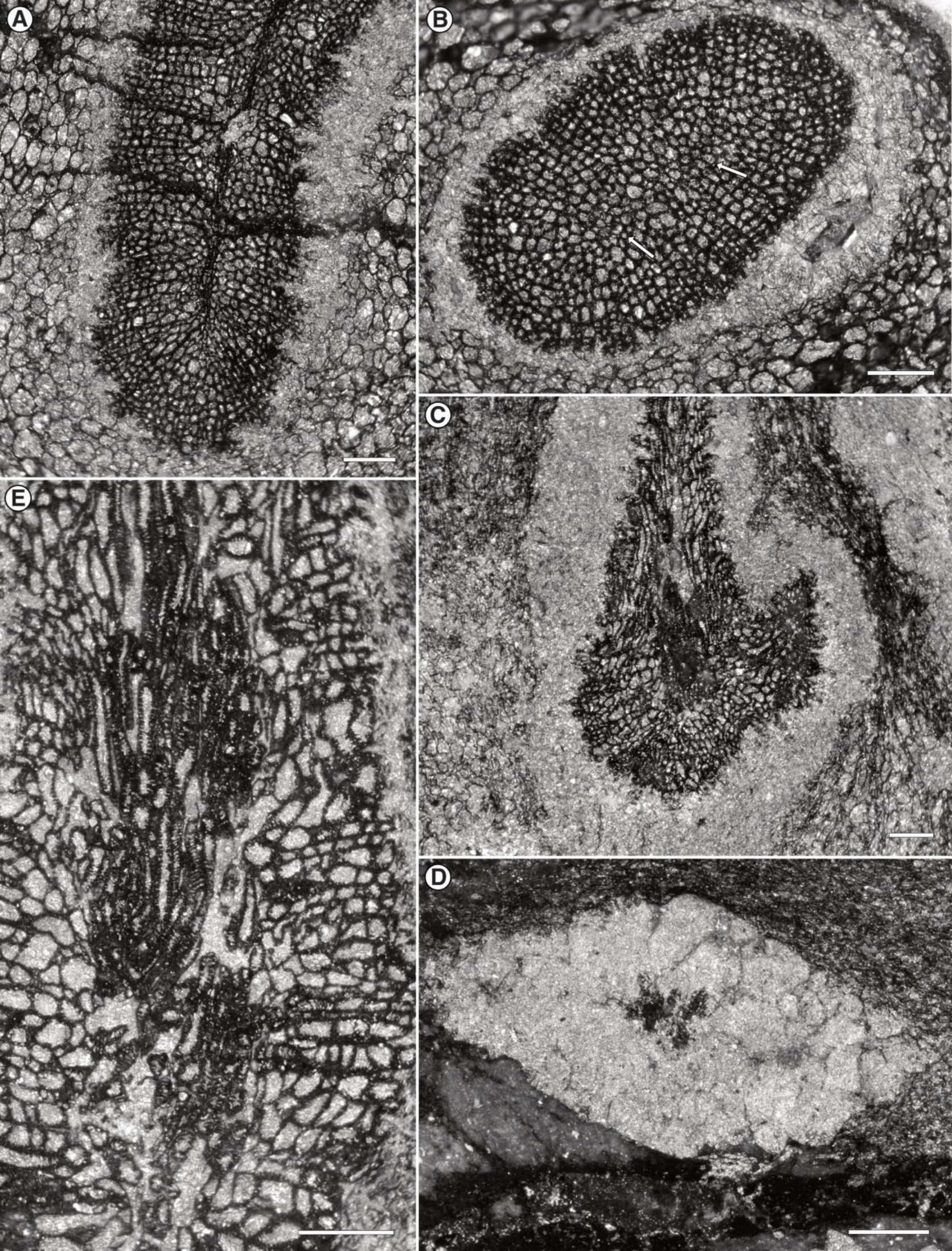
A
B
C
D
E

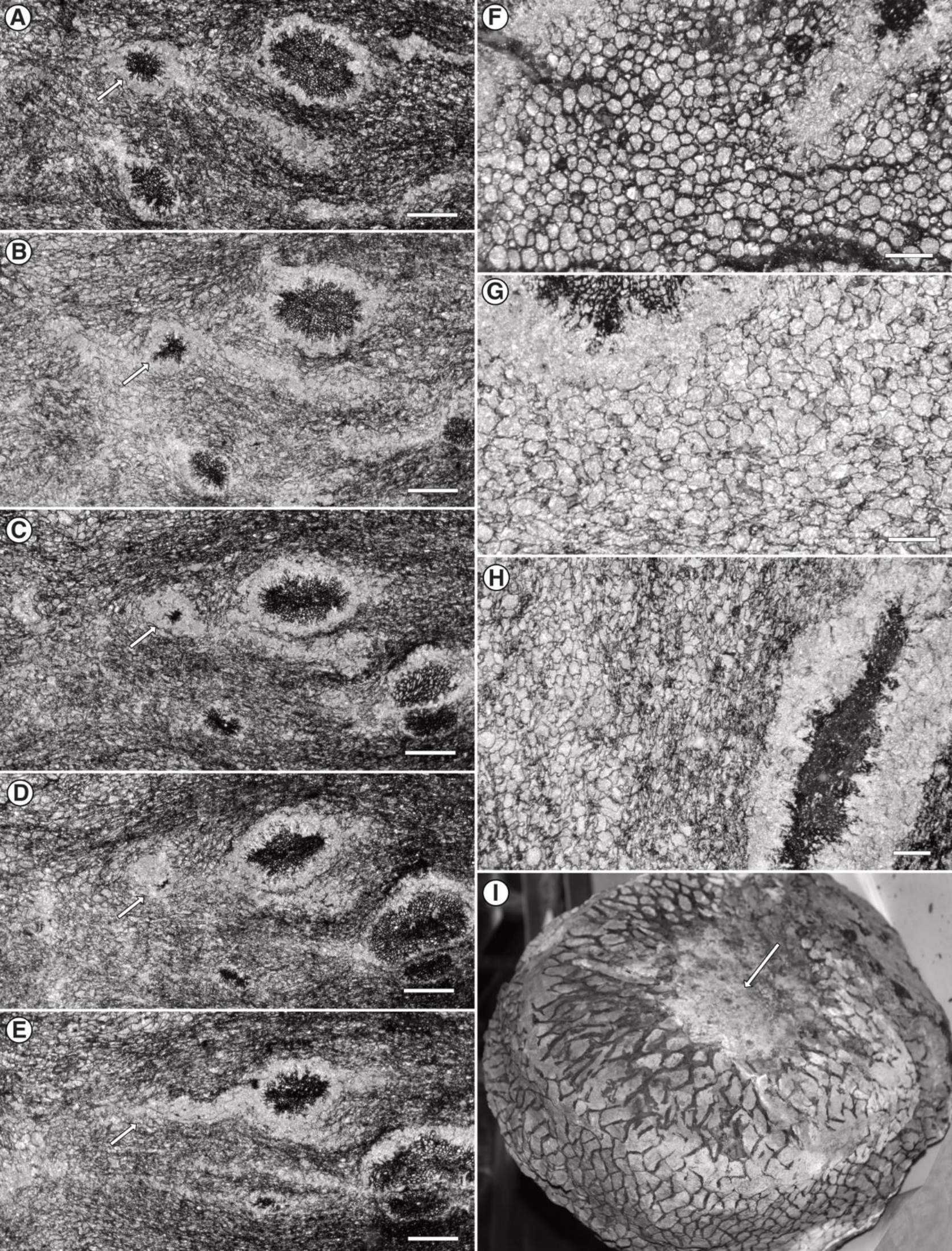
A
B
C
D
E
F
G
H
I

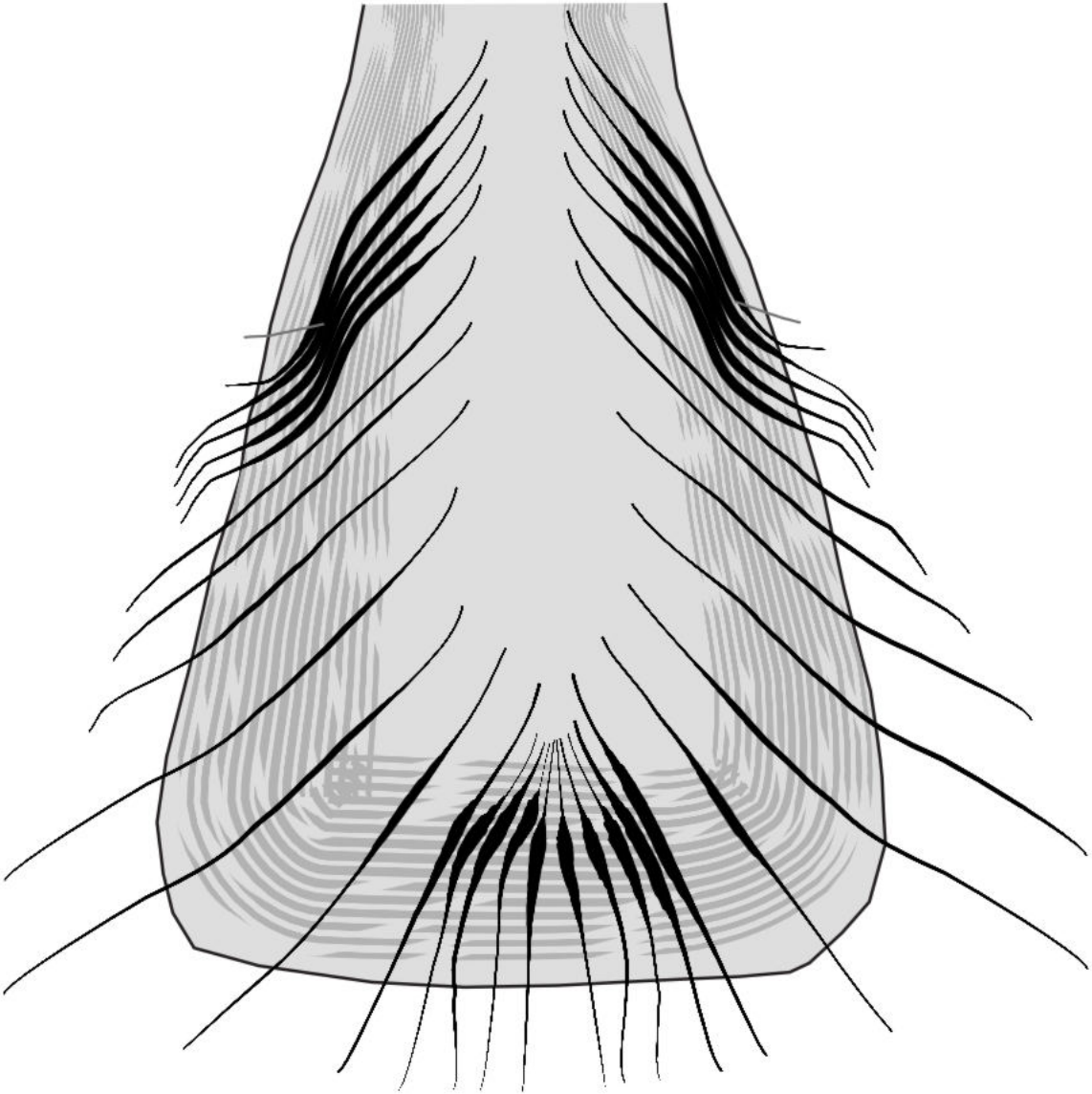

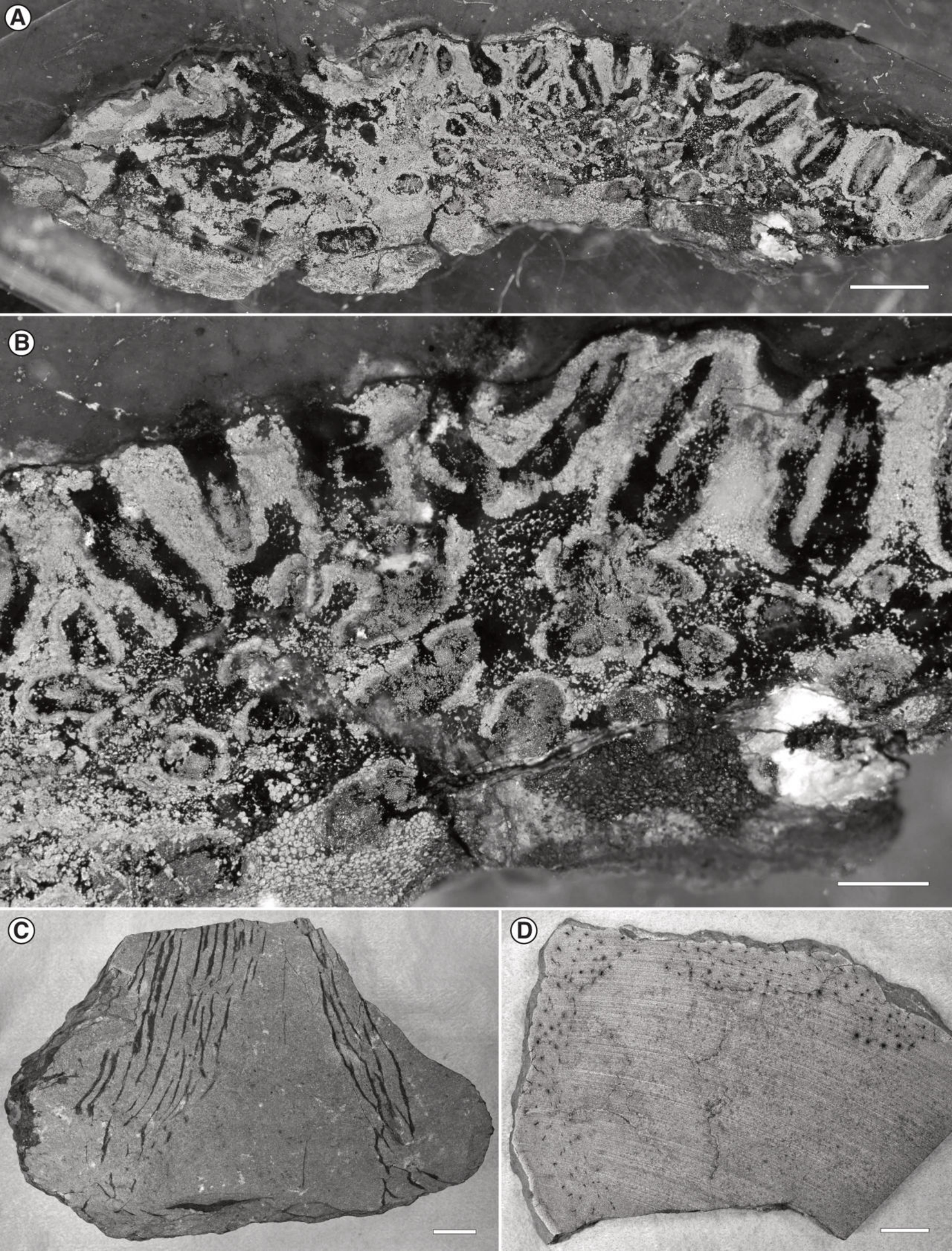
A
B
C
D

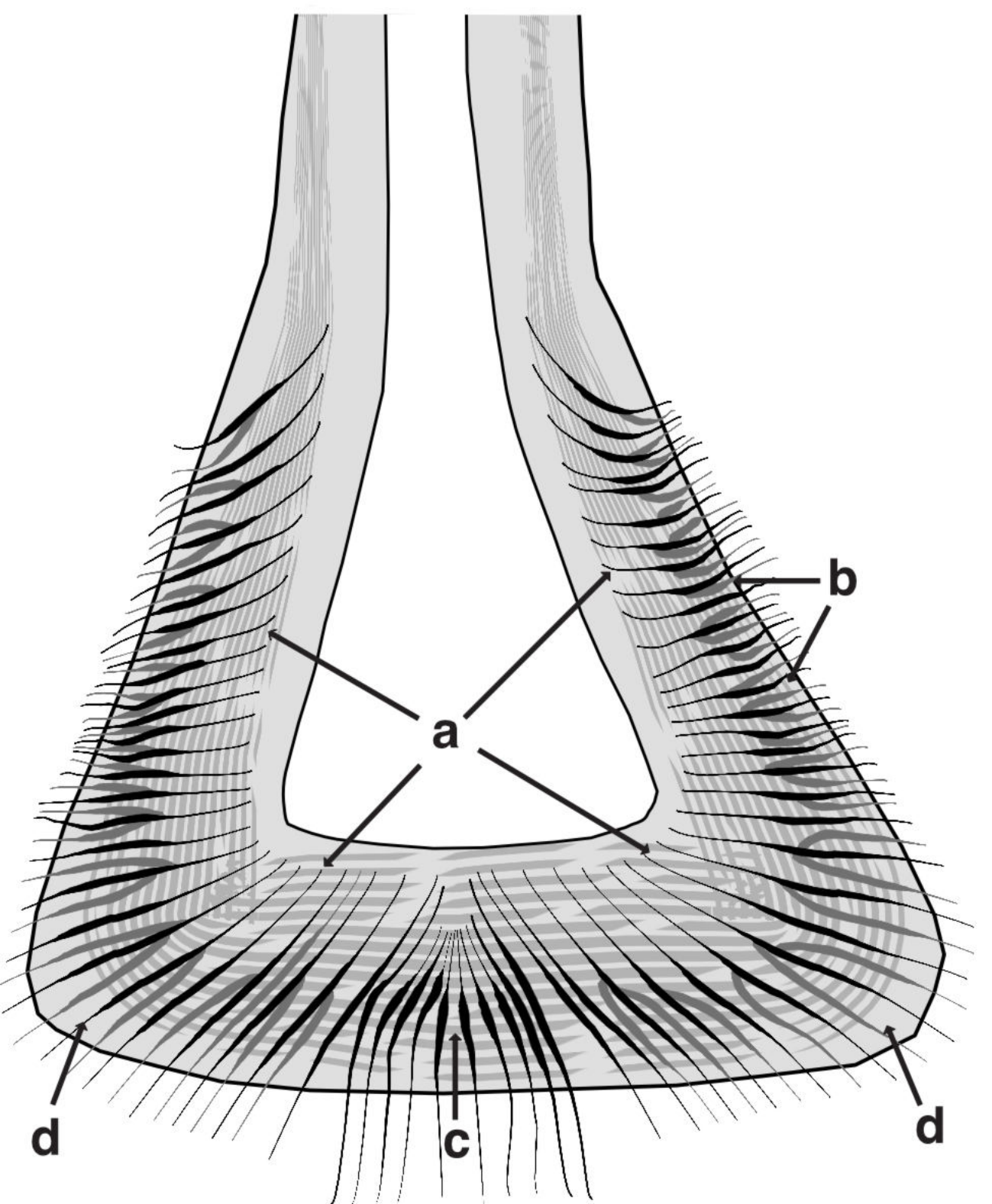
b
a
d
c
d